Nonprogressive Autosomal Recessive Ataxia Maps to Chromosome 9q34-9qter in a Large Consanguineous Lebanese Family

Valérie Delague, PhD,[1] Corinne Bareil, PhD,[2]
Patrice Bouvagnet, MD, PhD,[3] Nabiha Salem, MA,[1]
Eliane Chouery, MA,[1] Jacques Loiselet, MD, PhD,[1]
André Mégarbané, MD, PhD,[1] and
Mireille Claustres, MD, PhD[2]

Congenital ataxias are a heterogeneous group of predominantly nonprogressive disorders characterized by hypotonia, developmental delay followed by the appearance of ataxia, and often associated with dysarthria, mental retardation, and atrophy of the cerebellum. We performed a genome-wide screen on a large inbred Lebanese family presenting a nonprogressive autosomal recessive congenital cerebellar ataxia associated with short stature (MIM 213200), already described by Mégarbané and colleagues. The disease locus was assigned to a 12.1 cM interval on chromosome 9q34-9qter between D9S67 and D9S312. Differential diagnosis with other hereditary ataxias linked to the same region is discussed.

Ann Neurol 2001;50:250–253

Hereditary congenital ataxic disorders are a complex group of neurological disorders that manifests in infancy with abnormal motor development, hypotonia, delayed ability to sit and stand, and marked truncal ataxia. Dysarthria, mental retardation, and atrophy or hypoplasia of the cerebellum are almost always present as well.[2] Most of these cerebellar ataxias are nonprogressive, of which a half are of autosomal recessive transmission. As biochemical etiology is usually unknown and pathophysiology is poorly understood, the identification of genes will be important for a better classification and consequently early prognosis of these diseases.

We have recently identified a large inbred Lebanese family with autosomal recessive nonprogressive, gradually slightly improving, congenital cerebellar ataxia associated with short stature,[1] and hereby describe our results of a genome-wide search that allowed the assignment of a new disease locus on chromosome 9q34-9qter using identity by descent (IBD) and DNA pooling. The differential diagnosis of this syndrome with other ones linked to the same chromosomal region is discussed.

From the [1]Unité de Génétique Médicale, Laboratoire de Génétique Moléculaire, Faculté de Médecine, Université Saint-Joseph, Beirut, Lebanon; [2]Laboratoire de Génétique Moléculaire, Institut de Biologie, Montpellier, France; and [3]Laboratoire de Génétique Moléculaire Humaine, Université Claude Bernard, Lyon, France.

Received for publication Feb 19, 2001, and in revised form Apr 12. Accepted for publication Apr 12, 2001.

Address correspondence to Dr Mégarbané, Unité de Génétique Médicale. Faculté de Médecine, Université Saint-Joseph, 42, rue de Grenelle. 75007 Paris, France. E-mail: megarban@dm.net.lb

Patients and Methods

Patients

Thirty-two members of a Lebanese Maronite family had been previously investigated for hereditary nonprogressive cerebellar ataxia and short stature[1] (Fig 1). Briefly, the 12 affected members presented with a delay in psychomotor development, mild to severe ataxic gait and dysarthria, increased osteotendinous reflexes, hypotonia and/or spasticity, slightly diminished muscle strength, flat feet, short stature ranging from $<$10th to $<$3rd percentile, moderate to severe mental retardation, and defective orientation. The MRI showed pronounced cerebellar vermis and bilateral hemisphere hypoplasia, a dilated fourth ventricle, and a large cisterna magna.

Molecular Genetics Analysis

DNA POOLING AND HOMOZYGOSITY MAPPING. After familial investigations, EDTA blood samples were collected for genetic studies. DNA was extracted from lymphocytes by standard methods after informed consent was obtained from all adults and parents of children. Because all the patients included in the study were born to consanguineous marriages, we assumed identity by descent (IBD) and performed homozygosity mapping.[3] Three separate DNA pools were prepared by mixing equimolar quantities of individual DNA: the "affected" pool, the "obligate carrier" pool, and the "unaffected" pool. A genome-wide screening was conducted on theses three DNA pools as previously described.[4]

MICROSATELLITE ANALYSIS. The screening set comprised 400 highly polymorphic fluorescent-labeled markers from the ABI PRISM Linkage Map Set (version 2.0, PE Applied Biosystems) chosen from the Généthon linkage map[5] with an average spacing of 10–20 cM. PCR reactions and analysis of PCR products were performed as previously described by Delague and colleagues.[4] Alleles observed in the pedigree were numbered arbitrarily for each marker.

LINKAGE CALCULATIONS. Parametric linkage analysis was performed with the LINKAGE package 5.2.[6] Pairwise lodscores and multipoint lodscores were calculated using programs from FASTLINK 3.0P. The disease was assumed to be caused by a fully penetrant, autosomal recessive gene with a frequency of 0.002. As previous studies on genetic markers in Lebanon had shown that the Lebanese population is clearly Caucasian, with some Asian traits,[7] allele frequencies used in the calculations were those defined by Généthon in the Caucasian population and reported in the Genome Database. Marker order was chosen from the comprehensive genetic map of chromosome 9[8] and genetic distances from the

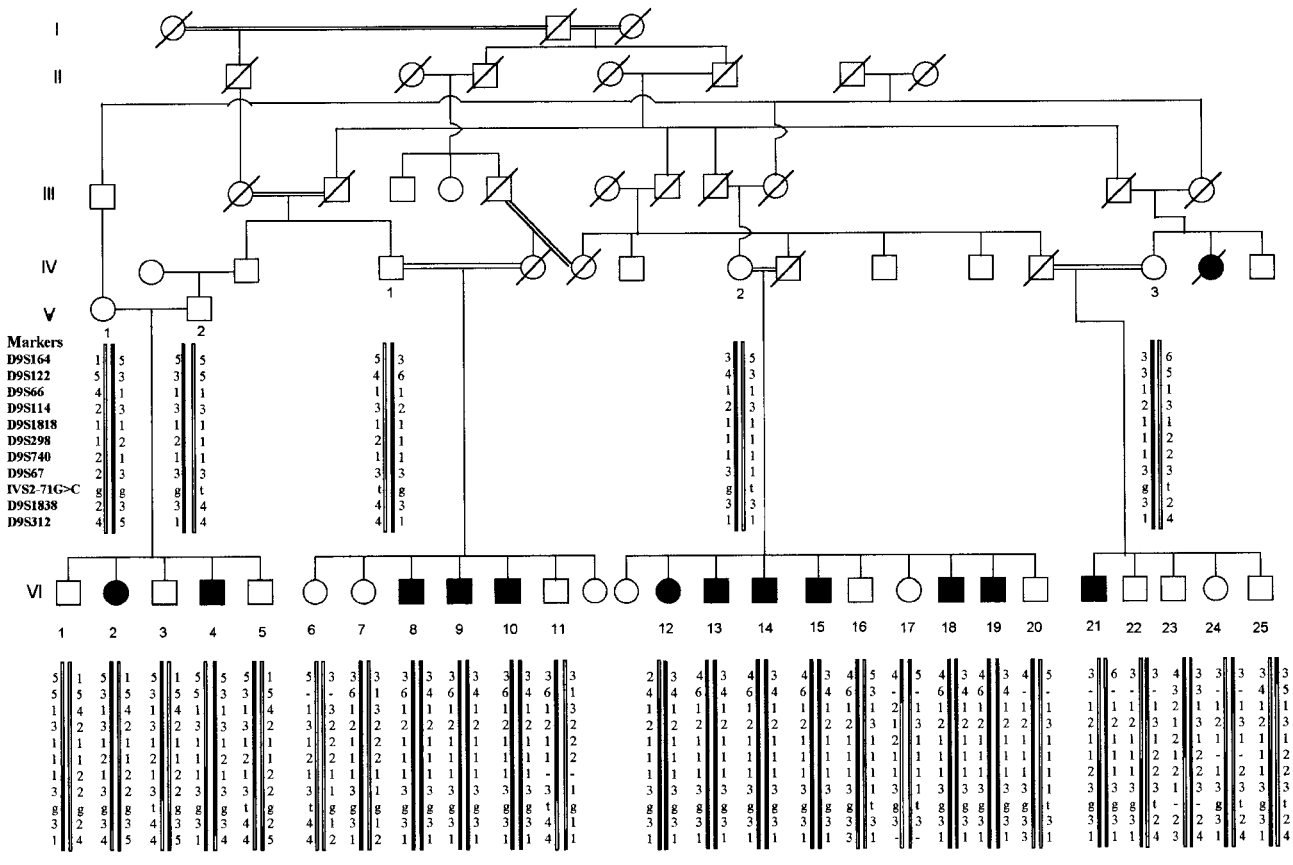

*Fig 1. Haplotype reconstruction in a consanguineous Lebanese family affected with a recessive nonprogressive cerebellar ataxia of Norman type at 9q34-qter. Markers are reported from centromere (*top*) to telomere (*bottom*). IVS2-71G>T describes a polymorphism in the intron 2 of* LHX3 *gene. Blackened symbols represent affected individuals. Disease-bearing chromosome is represented in black. Nontested markers are represented by a small dash (-).*

Galton Lab Comprehensive map (http://www.gene.ucl.ac.uk/public-files/chr9/genetic_maps/galton.map.comprehensive.txt). Considering that some of the genetic distances were not available in any of the integrated genetic maps, some of them were calculated in other pedigrees (data not shown).

SEQUENCING OF THE *LHX3* CODING REGION. The seven exons of the *LHX3* gene reported by Sloop and colleagues[9] were sequenced after PCR amplification using intronic primers designed from the following sequences: AF156888, AF188738, AF214637, AF188739, AF096165, AF188740, AF096166, AF188741, AF188742, AF096167, AF188743, and AF096168. Purified PCR products were sequenced in both directions with the use of the Big Dye Terminator Cycle Sequencing Ready Reaction kit on an ABI 377 sequencer (PE Biosystems). Electrophoregrams were analyzed using Sequence Analysis 3.3 and Sequence Navigator 1.0.1 softwares (PE Biosystems).

Results

Molecular genetic analysis

The genome-wide screening conducted on DNA pools allowed the rapid selection of several zones of homozygosity. Indeed, given the close consanguinity in the parents and the spacing of the markers, we assumed that at least one marker from the linked region would be homozygous in the "affected" DNA pool and not in the two other pools. In our pedigree, the consanguinity rate was so high that most of the locations showing a shift toward heterozygosity in the "affected" pool also showed this shift in the "obligate carrier" and the "unaffected" DNA pools. Genotyping with one or two distal and proximal markers allowed most regions to be excluded from linkage. Only an 18.4 cM region telomeric to D9S164 (AFM122xf4) appeared to be linked to the disease. In this region, genotyping was performed in each of the 32 individuals of the pedigree with eight additional markers. The *LHX3* gene, a LIM homeodomain transcription factor important for motor neuron specification and development of the pituitary gland had been considered a candidate gene for Joubert syndrome,[11] so it was screened for mutations in our family. No base change was identified, nevertheless, the IVS2-71G>T single nucleotide polymorphism (SNP) was used as bi-allelic polymorphic marker in the whole pedigree, instead of the uninformative microsatellite

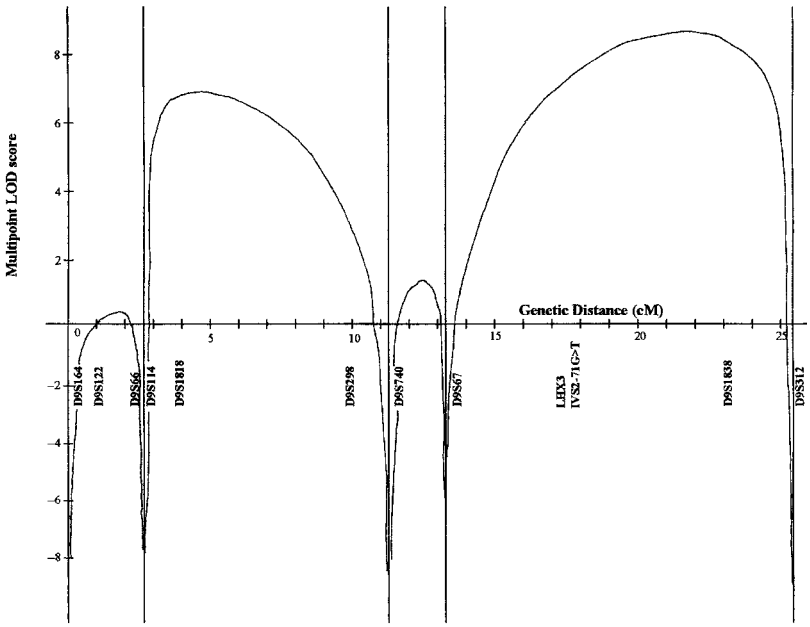

Fig 2. Results of multipoint LOD-score analysis of the disease locus at 9q34-9qter between markers D9S164 (centromeric) and D9S312 (telomeric). The y axis represents the multipoint lodscore (log10 value), and the x axis represents the genetic distance along the interval.

D9S158 (AFM073yb11), as *LHX3* was found to be located in the same clone (Genbank accession number: AL138781). Because of consanguinity, many markers were not fully informative, especially in the largest branch of the family (individuals VI-12 to VI-20), where almost all markers were noninformative (Fig 1). Nevertheless, in the rest of the family, haplotype analysis was consistent with linkage of the disease to this locus. Finally, the candidate region was restricted to an approximate 12.1 cM region on 9q34-9qter between D9S67 and D9S312 (Fig 1).

Lodscores calculations gave a maximal pairwise lodscore of 4.78 at $\Theta = 0.001$ and a maximum multipoint lodscore of 7.92 at $\Theta = 0.001$ (Fig.2) for the marker D9S1838 (AFMb303zg9), strongly supporting the linkage of the disease gene to the above region.

Discussion

A family presenting with autosomal recessive nonprogressive congenital ataxia was reported by Mégarbané and colleagues.[1] It is classified in the OMIM database in the heterogeneous group of Cerebellar Ataxia 1 or cerebelloparenchymal disorder III, where mental deficiency and cerebellar ataxia are congenital (MIM 213200). Although neuropathological studies were not performed in our patients, they all shared characteristics with the autosomal recessive Norman cerebellar atrophy, also known as the primary granular cell atrophy of the cerebellum.[10] As short stature associated with cerebellar ataxia has never been described so far in cases of Norman's disease, two hypotheses may be considered. Either short stature is not part of the syndrome and the association with cerebellar ataxia is the result of fortuitous segregation of two independent genes, because of the high level of consanguinity in this pedigree; or the family analyzed in this study presents an unpreviously described type of nonprogressive cerebellar ataxia, this new type being either allelic or nonallelic with the nonprogressive Norman's disease. The genome-wide screening conducted in this family allowed the localization of the disease gene on a 12 .1 cM region on 9q34-9qter between D9S67 and D9S312.

Recently, another autosomal recessive cerebellar ataxia, the Joubert syndrome (MIM 213300) has been mapped to 9q34.3[11] (Fig 3). The Lebanese patients shared clinical manifestations with Joubert syndrome: cerebellar vermis hypoplasia, hypotonia, and developmental delay. Nevertheless, they did not present abnormal breathing patterns nor abnormal eye movements, which are characteristic of Joubert syndrome.[12] Also, the characteristic appearance of Joubert syndrome patients was not observed in our patients, neither the typical "molar tooth sign" on neuroimaging of the head.[13] Thus, the possibility that they were affected with Joubert syndrome was excluded.

Two other loci were also recently assigned to the same chromosomal region: one locus for ataxia with oculomotor apraxia (AOA)[14] and the second one for spinocerebellar ataxia with cerebellar atrophy and peripheral neuropathy.[15] AOA (MIM 208920) is an autosomal recessive neurodegenerative disorder characterized by ataxia, oculomotor apraxia, and choreoathetosis—a clinical presentation different from the family reported herein. Its locus has been mapped to a 15.9 cM interval at 9q34, proximal to the one we located.

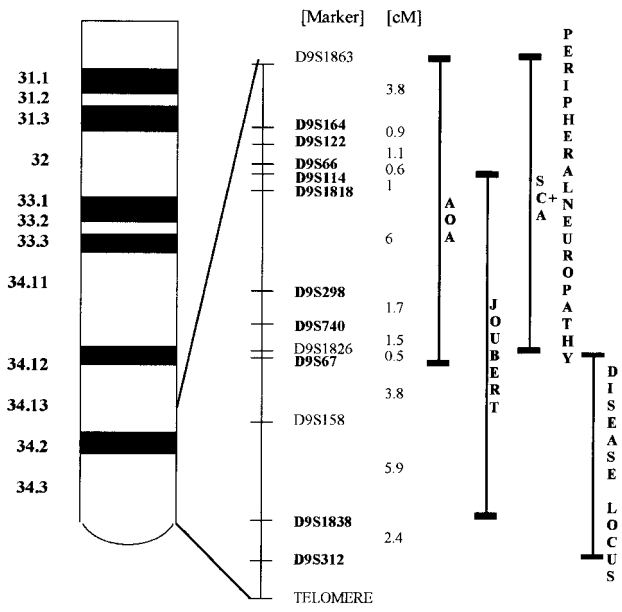

Fig 3. Schematic representation of the disease locus, showing the location of markers and the overlap between our candidate locus, Joubert's syndrome locus,[11] AOA locus,[14] and SCA-polyneuropathy locus.[15] Marker order is taken from the comprehensive genetic map of chromosome 9 reported by Povey and colleagues[8] and genetic distances from the Galton Lab Comprehensive map (http: / /www.gene.ucl.ac.uk/public-files/chr9/genetic_maps/galton.map.comprehensive.txt).

Patients affected by spinocerebellar ataxia with cerebellar atrophy and peripheral neuropathy[15] also present clinical signs that are not present in the Lebanese patients. Furthermore, the 20 cM genetic interval for this disease, located between D9S1863 and D9S158, is proximal to the one we located (Fig 3).

Thus, we have mapped a nonprogressive autosomal recessive cerebellar ataxia at a 12.1 cM interval at 9q34-9qter. As at least three other different types of ataxic syndromes, and *Barhl1*, a gene belonging to the new *bar* subfamily of mammalian homeobox genes and expressed in migrating neurons of the central nervous system,[16] map to the same chromosomal region on 9q34-9qter; we might postulate the presence of a cluster of homeobox genes involved in neurogenesis, resulting from duplications during evolution.[17] Further investigations will be needed in this family and in other pedigrees presenting nonprogressive cerebellar ataxia to identify the genes responsible for these diseases, allowing a better classification and early prognosis for these diseases.

We acknowledge the Institut Electricité-Santé de France and Alsthom for their donations to the Laboratoire de Génétique Moléculaire (Montpellier), and the Université Saint-Joseph for financially supporting VD's fellowship. The technical part of the work was supported by grants from the Jérôme Lejeune Foundation and the Laboratoire de Génétique Moléculaire (Montpellier).

We are grateful to the members of the family who were always very cooperative. Special thanks to Professor G. Lefranc for his continuous help and encouragement, and to Dr. Salim Adib for his technical help.

References

1. Mégarbané A, Delague V, Salem N, Loiselet J. Autosomal recessive congenital adrenal cerebellar hypoplasia and short stature in a large inbred family. Am J Med Genet 1999;87:88–90.
2. Harding A. Hereditary ataxias and related disorders. In: Ashbury, McKhan, McDonald, editors. Diseases of the nervous system: Clinical neurobiology. Volume 2, 2nd edition. Philadelphia: WB Saunders Company, 1992:1169–1178.
3. Lander E, Botstein D. Homozygosity mapping: a way to map human recessive traits with the DNA of inbred children. Science 1987;236:1567–1570.
4. Delague V, Bareil C, Tuffery S, et al. Mapping of a new locus for autosomal recessive demyelinating Charcot-Marie-Tooth disease to 19q13.1–13.3 in a large consanguineous Lebanese family: exclusion of MAG as a candidate gene. Am J Hum Genet 2000;67:236–243.
5. Dib C, Faure S, Fizames C, et al. A comprehensive genetic map of the human genome based on 5,264 microsatellites. Nature 1996;380:152–154.
6. Lathrop G, Lalouel J, Julier C, Ott J. Multilocus linkage analysis in humans: detection of linkage and estimation of recombination. Am J Hum Genet 1985;37:482–498.
7. Lefranc G, Rivat G, Serre J, et al. Common and uncommon immunoglobulin haplotypes among Lebanese communities. Hum Genet 1978;41:197–209.
8. Povey S, Attwood J, Chadwick B, et al. Report on the fifth international workshop on chromosome 9. Ann Hum Genet 1997;61:183–206.
9. Sloop K, Showalter A, Von Kap-Herr C, et al. Analysis of the human LHX3 neuroendocrine transcription factor gene and mapping to the subtelomeric region of chromosome 9. Gene 2000;245:237–243.
10. Norman RM. Primary degeneration of the granular layer of the cerebellum: an unusual form of familial cerebellar atrophy occurring in early life. Brain 1940;63:365–379.
11. Saar K, Al-Gazali L, Sztriha L, et al. Homozygosity mapping in families with Joubert syndrome identifies a locus on chromosome 9q34.3 and evidence for genetic heterogeneity. Am J Hum Genet 1999;65:1666–1671.
12. Sztriha L, Al-Gazali LI, Aithala GR, Nork M. Joubert's syndrome: new cases and review of clinicopathologic correlation. Pediatr Neurol 1999;20:274–281.
13. Maria B, Boltshauser E, Palmer S, Tran T. Clinical features and revised diagnostic criteria in Joubert syndrome. J Child Neurol 1999;14:590–591.
14. Németh AH, Bochukova E, Dunne E, et al. Autosomal recessive cerebellar ataxia with oculomotor apraxia (Ataxia-telangiectasia-like syndrome) is linked to chromosome 9q34. Am J Hum Genet 2000;67:1320–1326.
15. Bomont P, Watanabe M, Gershoni-Barush R, et al. Homozygosity mapping of spinocerebellar ataxia with cerebellar atrophy and peripheral neuropathy to 9q33–34, and with hearing impairment and optic atrophy to 6p21–23. Eur J Hum Genet 2000;8:986–990.
16. Bulfone A, Menguzzato E, Broccoli V, et al. Barhl1, a gene belonging to a new subfamily of mammalian homeobox genes, is expressed in migrating neurons of the CNS. Hum Mol Genet 2000;9:1443–1452.
17. Schughart K, Kappen C, Ruddle F. Duplication of large genomic regions during the evolution of vertebrate homeobox genes. Proc Nat Acad Sci U S A 1989;86:7067–7071.

Levodopa Induces Dyskinesias in Normal Squirrel Monkeys

Daniel M. Togasaki, MD, PhD, Louis Tan, MRCP, Peter Protell, BA, Donato A. Di Monte, MD, Maryka Quik, PhD, and J. William Langston, MD

This study assessed whether or not levodopa induces dyskinesias in normal (ie, unlesioned) squirrel monkeys. All six animals treated twice daily with levodopa (15 mg/kg with carbidopa by oral gavage) for two weeks developed choreoathetoid dyskinesias, whereas none of the vehicle-treated animals displayed any abnormal movements. These dyskinesias did not merely reflect a generalized motor activation as locomotion was actually suppressed. The present data demonstrate that preexisting nigrostriatal damage is not necessary for the development of levodopa-induced dyskinesias.

Ann Neurol 2001;50:254–257

A substantial body of evidence suggests that preexisting nigrostriatal damage is required for the development of levodopa-induced dyskinesias. For example, there are numerous reports of nonparkinsonian individuals who were treated with levodopa, sometimes for years, without developing dyskinesias.[1–3] In contrast, patients with Parkinson's disease are clearly at risk for developing this complication of chronic levodopa therapy.[4] These clinical observations have been mirrored by numerous studies of nonhuman primates in which normal animals treated with levodopa failed to develop dyskinesias[5–9] but animals with parkinsonism induced by 1-methyl-4-phenyl-1,2,3,6-tetrahydropyridine quickly developed these abnormal movements.[6,9–11] There have been a handful of reports suggesting that dyskinesias may be caused by levodopa in the absence of nigrostriatal damage in normal primates[12–15] as well as in nonparkinsonian patients.[16,17] These studies, however, were neither controlled nor prospective in design to specifically address this important issue. We now report the results of such an investigation.

From The Parkinson's Institute, Sunnyvale, CA.

Received Dec 11, 2000, and in revised form Apr 23, 2001. Accepted for publication May 4, 2001.

Address correspondence to Dr Togasaki, The Parkinson's Institute, 1170 Morse Avenue, Sunnyvale, CA 94089.
E-mail: dtogasaki@parkinsonsinstitute.org

Material and Methods

Animals and Drug Treatment

Ten healthy, drug-naive squirrel monkeys *(Saimiri sciureus)* were used for this study. Animals were young adults, as judged by dentition, and weighed 0.629 to 0.775 kg. All work conformed to the guidelines of the United States Public Health Service's *Policy on Humane Care and Use of Laboratory Animals* and was approved by our Institutional Animal Care and Use Committee.

Monkeys were treated with levodopa and carbidopa (15 and 3.75 mg/kg, respectively) or vehicle by orogastric gavage twice daily at 9:00 AM and 1:00 PM. Levodopa solutions were prepared immediately prior to administration from thoroughly crushed tablets of Sinemet CR (DuPont Pharma, Wilmington, DE). Animals were treated for 5 days, rested for 2 days, then were treated for 5 additional days. They had free access to water and received food (without protein) immediately after the second treatment of the day and a full meal at the end of the day.

Behavioral Observation

Animals were videotaped each treatment day for 9 hours, starting 1 hour before their first dose of drug or vehicle (baseline). Two independent raters, blinded to treatment, observed the videotaped recordings for 2-minute periods at 20-minute intervals. The severity of the dyskinetic movements was assessed using the Global Primate Dyskinesia Rating Scale[18] (GPDRS). This scale ranges from 0 (no abnormal movements) to 4 (severe and incapacitating). Locomotor activity was measured in cages fitted with infrared activity monitors[19] (IRAMs) by counting the times a monkey interrupted infrared beams traversing its cage. Beams were spaced 2 body widths apart; to register a count, the animal had to break a beam different from the one just broken.

Data Analysis

The presence of choreoathetoid movements in the 2 groups was compared by χ^2 analysis. An average daily dyskinesia time course of the dyskinesia ratings was constructed for each animal by averaging all 10 of that animal's daily time courses into a single curve. These time courses were analyzed by repeated-measures analysis of variance (ANOVA), with the between-groups factor being treatment (levodopa vs. vehicle) and the within-groups factors being dose time (morning vs. afternoon) and time after dose (every 20 minutes from 0 to 240 minutes).

The IRAM count for the 10-minute session prior to each dyskinesia rating was averaged together with that of the 10-minute session following the rating, to provide activity counts that corresponded with 20-minute intervals. These averaged counts were then used to construct average daily locomotor activity time courses, which underwent the same analysis as the dyskinesia ratings. GPDRS dyskinesia ratings were correlated with IRAM counts ($n = 1{,}302$): a correlation coefficient was calculated and its significance (against $r = 0$) was tested using Fisher's R to z transformation.

Statistical analyses were performed using *StatView* version 5.0.1 (SAS Institute, Cary, NC); a significance level of 0.05 was used.

Results

Dyskinesias

All 6 normal squirrel monkeys treated with levodopa developed choreoathetoid dyskinesias, whereas the 4 vehicle-treated animals never scored above 0 on the GPDRS (χ^2 $p = 0.0016$). Although the severity of the dyskinesias changed over different days, the basic phenomenology did not. These changes were reflected, quantitatively and qualitatively, in the dyskinesia ratings. These changes followed a typical course of progression after a dose of levodopa. The initial abnormal behavior observed was swaying and rocking, which gradually intensified until it was continuous. Next, choreoathetoid movements appeared and then increased in intensity. The arms were affected more than the legs in the initial stages, but eventually the choreoathetoid movements spread to all 4 limbs.

Dyskinesia ratings for the 2 experimental groups treated with levodopa or vehicle are shown in Figure 1. The first observation of abnormal movements occurred

Fig 1. Average dyskinesia ratings for normal monkeys treated with levodopa 15 mg/kg twice daily (open circles, n = 6) or an equivalent amount of water (solid circles, n = 4). Monkeys were observed for 1 hour as a baseline, then for 4 hours after the first treatment, followed by the second treatment and another 4 hours of observation. Values are means ± SEM.

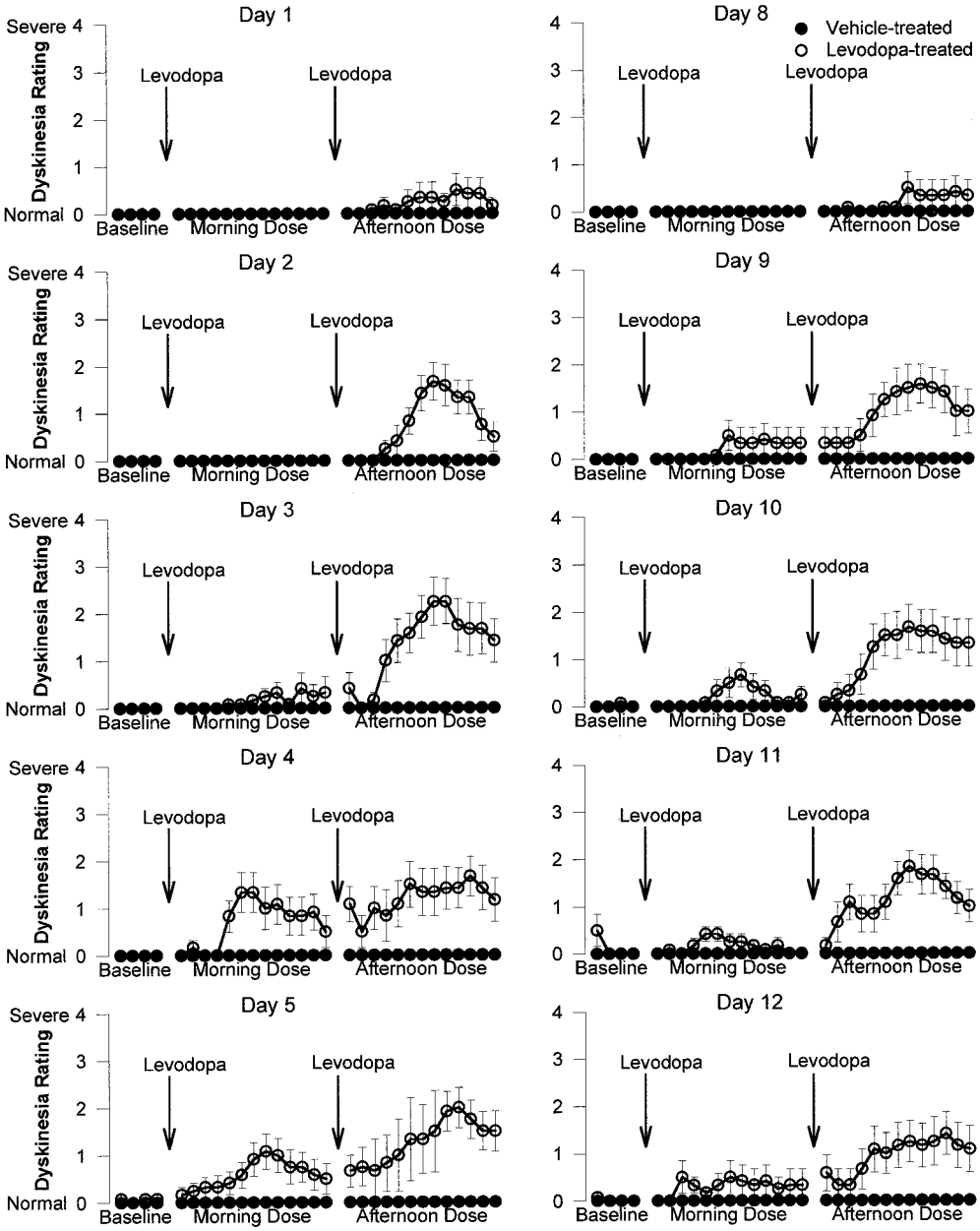

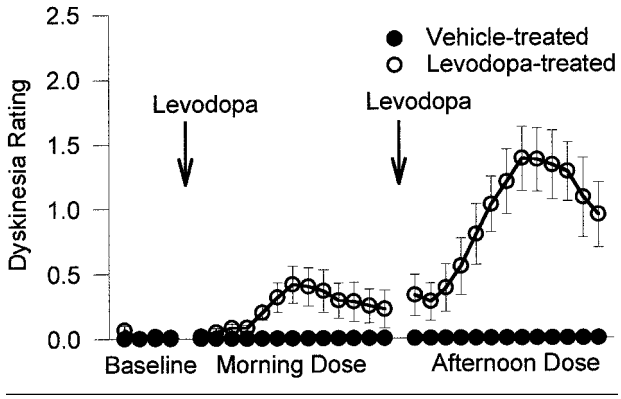

*Fig 2. Average dyskinesia ratings across all treatment days (average daily dyskinesia time course) for normal monkeys treated with levodopa 15 mg/kg twice daily (*open circles*, n = 6) or an equivalent amount of water (*solid circles*, n = 4). The 2 treatment groups were different (*p = *0.0149), and dyskinesia ratings were higher following the afternoon dose than following the morning dose (*p = *0.0026). Values are means ± SEM of each monkey's average values.*

after the afternoon dose on experimental day 1 (2 animals), day 2 (3 animals) or day 8 (1 animal). Abnormal movements began appearing after the morning dose on day 3 (2 animals), day 4 (2 animals) and day 9 (2 animals).

The average daily dyskinesia time courses of the levodopa-treated group, as illustrated in Figure 2, differed from those of vehicle-treated animals (ANOVA $F = 9.537$, $p = 0.0149$). Dyskinesia ratings were higher after the afternoon than after the morning dose of levodopa (significant interaction between dose time and treatment by ANOVA: $F = 18.584$, $p = 0.0026$). Average ratings reached a maximum at 120 to 140 minutes after levodopa administration and did not return to 0 by the end of either the morning or afternoon session.

Locomotor Activity

After dosing, IRAM counts for levodopa-treated animals decreased, then gradually returned to control levels (Fig 3). This occurred after both doses on each treatment day. Vehicle-treated animals had relatively constant IRAM counts, indicating that the gavage procedure did not affect locomotion. Time courses were different between the 2 groups (significant interaction between time and treatment by ANOVA: $F = 2.280$, $p = 0.0135$). The decrease in IRAM counts contrasted with the increase in dyskinesia ratings, and there was no correlation between these 2 parameters ($r = 0.05$, $p = 0.0698$).

Discussion

Using a scale that has been characterized for reliability and validity[18] and raters who were blinded to treatment status, all levodopa-treated monkeys were observed to develop dyskinesias, whereas control monkeys never developed abnormal movements. Thus, these results clearly show that levodopa-induced dyskinesias do not require preexisting nigrostriatal damage. The movements seen in the dyskinetic animals were identical to those in monkeys with nigrostriatal lesions and highly reminiscent of those seen in humans. Quantitative locomotor monitoring ruled out the possibility that the dyskinesias were simply the result of generalized motor activation. Indeed, locomotion was actually decreased in levodopa-treated animals.

It is unclear why many previous studies failed to observe levodopa-induced dyskinesias in normal (i.e., unlesioned) animals.[5–9] It might be that species susceptibility is important, with squirrel monkeys being more sensitive to the effects of levodopa than either rhesus[8] or cynomolgus[5,9] monkeys. Two of the negative studies, however, involved squirrel monkeys. Possibly, the twice-daily oral administration of levodopa used here might be more effective than the intermittent single doses[6] or intraperitoneal injections[7] used in other studies. Furthermore, as noted earlier, our results are not completely unprecedented. Sassin and colleagues[15] observed dyskinesias in rhesus monkeys treated with levodopa (100 to 400 mg/kg daily). Both Paulson[13] and Mones[12] also reported dyskinesias in rhesus monkeys but only after huge (up to 660 mg/kg) and repeated

*Fig 3. Average infrared activity monitor (IRAM) counts across all treatment days (average daily locomotor activity time course) for normal monkeys treated with levodopa 15 mg/kg twice daily (*open circles*, n = 6) or an equivalent amount of water (*solid circles*, n = 4). IRAM counts were totaled for 10-minute intervals, and 2 scores were averaged for each 20-minute interval, except for the first and last observations of the baseline, morning, and afternoon periods, which were reported as the score for that 10-minute session. Monkeys were observed for 1 hour as a baseline, then for 4 hours after the first treatment, followed by the second treatment and another 4 hours of observation. Time courses for the 2 treatment groups differed significantly (*p = *0.0135). Values are means ± SEM of each monkey's average values.*

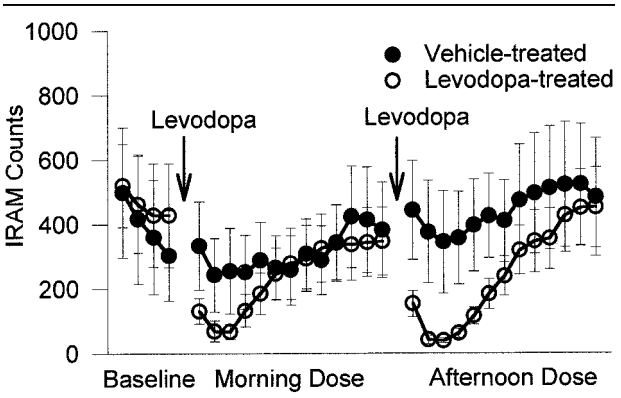

doses of levodopa. The interpretation of these studies is complicated by their use of drug regimens that were frankly toxic (sometimes lethal). Pearce[14] reported that eight of 16 cynomolgus monkeys treated with levodopa (80 mg/kg daily with carbidopa for 13 weeks) developed severe dyskinesias. This finding, however, still lacks documentation with behavioral data. Our work fills many of the gaps in these previous studies by using a well-tolerated dose of levodopa in a prospective, controlled behavioral investigation. The current results in squirrel monkeys therefore confirm and extend earlier work in rhesus and cynomolgus monkeys and clearly indicate that normal primates can develop typical levodopa-induced dyskinesias.

This study also provides several interesting observations regarding the temporal pattern of the evolution of dyskinesias. First, although dyskinesias were never seen with the first dose of levodopa, they did arise early in the course of twice-daily dosing (often within the first three days), a phenomenon that may be explained by exposure to relatively high levels of levodopa (equivalent to 2,000 mg daily in a human). Second, dyskinesias were more pronounced in the afternoon, an observation that is often reported by patients as well. Third, the severity increased over several days of treatment, perhaps reflecting accumulating dopamine stores. Fourth, the time course of development of abnormal movements did not appear to differ between the first and second treatment weeks. This finding might be a particular feature of dyskinesias induced by levodopa in the absence of nigrostriatal denervation since a brief "drug holiday" in parkinsonian patients typically does not reset their dyskinesias back to pretreatment levels.

The results reported here have important implications for the theory that nigrostriatal damage predisposes to the development of dyskinesias by impairing striatal "buffering" capability.[20] That dyskinesias can occur in unlesioned monkeys suggests either that the buffering mechanism is less important than previously thought or that sufficiently high doses of levodopa might be capable of overwhelming even an intact buffering system. On a more practical level, this model provides a new tool for the experimental investigation of levodopa-induced dyskinesias as most previous studies have been carried out on a background of changes induced by nigrostriatal denervation. Using this new model, we can now investigate the pharmacologic and molecular changes that occur in the brain of primates with levodopa-induced dyskinesias in the absence of such confounding factors, which in turn should lead to new insights for understanding this major complication of levodopa therapy.

This study was supported by the National Institutes of Health (grant NS34886-01A2) and the National Parkinson's Foundation. L.T. was supported by the National Medical Research Council-Singapore.

We thank Jeff McCorkle, Gerald Shrader, Cristobal San Nicolas, Evangelito Valdez, and Dr Joanne Blum for their assistance with the animals and Dr Louis E. DeLanney for helpful discussions.

References

1. Arts N, Van de Vlasakker C, Tacke T, Horstink M. Is l-dopa harmful? Lancet 1991;338:1210–1211.
2. Mones RJ, Elizan TS, Siegel GJ. Analysis of l-dopa induced dyskinesia in 51 patients with parkinsonism. J Neurol Neurosurg Psychiatry 1971;34:668–673.
3. Rajput AH, Fenton ME, Birdi S, Maculay R. Is levodopa toxic to human substantia nigra? Mov Disord 1997;12:634–638.
4. Nutt JG. Clinical pharmacology of levodopa-induced dyskinesia. Ann Neurol 2000;47(Suppl 1):S160–S164.
5. Alexander GM, Schwartzman RJ, Grothusen JR, et al. Changes in brain dopamine receptors in MPTP parkinsonian monkeys following l-dopa treatment. Brain Res 1993;625:276–282.
6. Boyce S, Rupniak NMJ, Steventon MJ, Iversen SD. Nigrostriatal damage is required for induction of dyskinesias by l-dopa in squirrel monkeys. Clin Neuropharmacol 1990;13:448–458.
7. Ng LKY, Gelhard RE, Chase TN, MacLean PD. Drug-induced dyskinesia in monkeys: a pharmacologic model employing 6-hydroxydopamine. In: Barbeau A, Chase TN, Paulson GW, eds. Advances in neurology, vol 1. New York: Raven, 1973: 651–655.
8. Sax DS, Butters N, Tomlinson EB, Feldman RG. Effects of serial caudate lesions and L-DOPA administration upon the cognitive and motor behavior of monkeys. In: Barbeau A, Chase TN, Paulson GW, eds. Advances in neurology, vol 1. New York: Raven, 1973:657–663.
9. Schneider JS. Levodopa-induced dyskinesias in parkinsonian monkeys: relationship to extent of nigrostriatal damage. Pharmacol Biochem Behav 1989;34:193–196.
10. Gomez-Mancilla B, Bedard PJ. Effect of D1 and D2 agonists and antagonists on dyskinesia produced by l-dopa in 1-methyl-4-phenyl-1,2,3,6-tetrahydropyridine–treated monkeys. J Pharmacol Exp Ther 1991;259:409–413.
11. Pearce RK, Jackson M, Smith L, et al. Chronic L-DOPA administration induces dyskinesias in the 1-methyl-4- phenyl-1,2,3,6-tetrahydropyridine–treated common marmoset (Callithrix jacchus). Mov Disord 1995;10:731–740.
12. Mones RJ. Experimental dyskinesias in normal rhesus monkey. In: Barbeau A, Chase TN, Paulson GW, eds. Advances in neurology, vol 1. New York: Raven, 1973:665–669.
13. Paulson GW. Dyskinesia in monkeys. In: Barbeau A, Chase TN, Paulson GW, eds. Advances in neurology, vol 1. New York: Raven, 1973:647–650.
14. Pearce RKB. l-Dopa and dyskinesias in normal monkeys. Mov Disord 1999;14(Suppl 1):9–12.
15. Sassin JF, Taub S, Weitzman ED. Hyperkinesia and changes in behaviour produced in normal monkeys by l-dopa. Neurology 1972;22:1122–1125.
16. Goodwin FK, Murphy DL, Brodie KH, Bunney WE. l-Dopa, catecholamines and behaviour: a clinical and biochemical study in depressed patients. Biol Psychiatry 1970;2:342–366.
17. Lieberman AN, Goodgold AL, Goldstein M. Treatment failures with l-dopa in parkinsonism. Neurology 1972;22:1205–1210.
18. Langston JW, Quik M, Petzinger G, et al. Investigating levodopa-induced dyskinesias in the parkinsonian primate. Ann Neurol 2000;47(Suppl 1):S79–S89.
19. Irwin I, DeLanney LE, Forno LS, et al. The evolution of nigrostriatal neurochemical changes in the MPTP-treated squirrel monkey. Brain Res 1990;531:242–252.
20. Chase TN. Levodopa therapy: consequences of the nonphysiologic replacement of dopamine. Neurology. 1998;50(Suppl 5): S17–S25.

Sporadic Creutzfeldt-Jakob Disease in a Young Dutch Valine Homozygote: Atypical Molecular Phenotype

Mark W. Head, PhD,[1] Gerrit Tissingh, MD,[2]
Bernard M. J. Uitdehaag, MD, PhD,[2]
Frederik Barkhof, MD, PhD,[3] Tristan J. R. Bunn, MSc,[1]
James W. Ironside, FRCP,[1]
Wouter Kamphorst, MD, PhD,[4] and
Philip Scheltens, MD, PhD[2]

A case of sporadic Creutzfeldt-Jakob disease (sCJD) is described in a young Dutch protein prion gene *(PRNP)* codon 129 valine homozygote. Certain clinical and molecular features of this case overlap those of variant CJD. The case highlights possible difficulties in the differential diagnosis of vCJD and the more rare sCJD subtypes based on molecular features alone.

Ann Neurol 2001;50:258–261

Creutzfeldt-Jakob disease (CJD) is a rare, rapidly progressive, and invariably fatal neurodegenerative condition characterised clinically by dementia and ataxia and pathologically by neuronal loss, gliosis, and spongiform change in the brain. It can be inherited (familial CJD), acquired (iatrogenic CJD), or idiopathic (sporadic CJD, sCJD). Irrespective of aetiology, CJD is characterised by the accumulation of an altered form (PrP^{Sc}) of a host-encoded glycoprotein (PrP^{C}). Mutations in the gene encoding PrP, termed *PRNP*, are closely associated with the inherited forms of the disease, whereas medical histories that include procedures such as human growth hormone treatment or dura mater grafting are strongly indicative of iatrogenic CJD. Susceptibility and disease phenotype can be substantially modified by the common methionine/valine polymorphism at codon 129 of *PRNP*.

In 1996, a new form of the disease, variant CJD (vCJD), was described in the United Kingdom,[1] which appears to result from infection with the bovine spongiform encephalopathy (BSE) agent.[2,3] vCJD patients are younger than sCJD patients and usually present with psychiatric symptoms, followed by ataxia, movement disorders, and dementia during a protracted disease course. The eventual size of the current epidemic of vCJD is uncertain, but accurate long-term predictions necessitate ongoing surveillance and accurate diagnosis. The phenotype described in the first 10 cases has proved consistent, allowing formulation of clinical diagnostic criteria for probable vCJD in living patients with strong predictive value.[4] The recent inclusion of a postthalamic high magnetic resonance imaging (MRI) signal (the pulvinar sign) has further strengthened the criteria.[4,5] Nevertheless, a definite diagnosis of vCJD requires neuropathological examination of the brain.[6] Another consistent finding in vCJD has been the presence in the brain of a predominantly diglycosylated form of the protease-resistant prion protein (PrP^{res}).[6–8] A further accentuation of this "glycosylation signature" in PrP^{res} was found in vCJD tonsil.[9] Thus far, all patients with a definite diagnosis of vCJD who have been tested have been methionine homozygotes at codon 129 of *PRNP*. This has prompted speculation concerning the possibility and potentially novel phenotype(s) of BSE infection in humans with valine at codon 129.[3,10]

In practice, sCJD is the major differential diagnosis of vCJD.[4] However, sCJD has a remarkably diverse clinicopathological phenotype. A recent study of 300 sCJD cases identified six distinct subtypes.[11] Each subtype correlated with a particular combination of PrP^{res} isotype, defined by the molecular size of the nonglycosylated, protease-resistant core fragment (type 1, 21 kDa, or type 2, 19 kDa) and *PRNP* codon 129 genotype (methionine homozygosity, MM; heterozygosity, MV; or valine homozygosity, VV). Two of the least frequent subtypes of sCJD require particular attention in relation to vCJD. First, the PrP^{res} in methionine homozygous type 2 (MM2) cases differ only in glycosylation site occupancy from the PrP^{res} found in vCJD. Second, the valine homozygous type 1 (VV1) sCJD subtype has a young age at onset and, in common with MM2 cases, a prolonged disease course. These clinical features alone may prompt neurologists to consider, perhaps inappropriately, a diagnosis of vCJD.

This report describes a case of sCJD in a valine homozygote, which brings several issues surrounding the differential diagnoses of vCJD and sCJD into sharp focus.

Case Presentation

A previously healthy 42-year-old woman was referred to the outpatient memory clinic of the Vrije University Medical Centre suffering from progressive memory

From the [1]National Creutzfeldt-Jakob Disease Surveillance Unit and Department of Pathology, University of Edinburgh, Western General Hospital, Edinburgh, UK; [2]Department of Neurology, [3]Department of Radiology, and [4]Department of Pathology, Vrije Universiteit Medical Center, Amsterdam, the Netherlands.

Received Dec 6, 2000, and in revised form May 9, 2001. Accepted for publication May 9, 2001.

Address correspondence to Dr Head, National CJD Surveillance Unit, Western General Hospital, Edinburgh, EH4 2XU, UK.
E-mail: m.w.head@ed.ac.uk

loss, spatial disorientation, depression, and headache over the previous 8-month period. Sensory and psychiatric features were not evident. The patient had no family history of dementia and no obvious iatrogenic exposure to prions and had been continuously resident in the Netherlands. On admission, neurological examination revealed global memory impairment, visual agnosia, visuospatial disturbances, mild cerebellar ataxia, and minor involuntary movements, best described as "fidgety." Clinical tests showed 14-3-3 positive cerebrospinal fluid and an absence of periodic sharp wave complexes on electroencephalography (EEG). MRI showed signal increase in the grey matter on diffusion-weighted images. No mutations were found in *PRNP*, but the patient was homozygous for valine at codon 129. Given the early age at onset and the already protracted disease course, a brain biopsy (right frontal cortex) was performed 2 months after admission, to confirm the provisional diagnosis of CJD and discount a diagnosis of vCJD. Neuropathological examination of this material showed transcortical microvacuolar spongiform change, variable neuronal loss, and gliosis (Fig 1A). No amyloid plaques were visible using Congo red or periodic acid-Schiff stains. PrP immunohistochemistry showed a diffuse granular "synaptic" pattern, with no plaques visible (Fig 1B). Western blot analysis showed easily detectable levels of PrP^{res}, with a 21 kDa nonglycosylated band (type 1) and an unremarkable glycoform ratio (Fig 2). Immunohistochemical and Western blotting studies were carried out exactly as described previously.[6] Taken together, these findings support a diagnosis of sCJD, the atypical clinical features of the case being consistent with the rare VV1 sCJD subtype.

Over the following months, the patient became akinetic and mute, with persistent mild ataxia (she was still able to walk 14 months after the first symptoms) and myoclonic jerks towards the end of the disease course. She died 18 months after the onset of symptoms. Permission for post-mortem examination was restricted to the brain. Histopathological examination of the left cerebral hemisphere, cerebellum, and brain stem showed pathology similar to that seen at biopsy: cerebral cortical spongiform change, more severe neuronal loss, and gliosis (Fig 1C), as well as a synaptic PrP immunostaining pattern and absence of plaques (Fig 1D). This histological appearance was typical of all cortical regions examined, with no laminar pattern of PrP deposition. Spongiform change was also present in the hippocampus. The caudate nucleus and putamen exhibited severe spongiform change, but this feature was less marked in the thalamus and brain stem. PrP immunocytochemistry showed granular synaptic staining in all of these regions, along with small numbers of PrP-positive plaque-like structures (which were not evident on routine microscopy). Patchy spongiform change was present in the cerebellar molecular layer, accompanied by Purkinje cell loss and gliosis. PrP deposition occurred in a granular synaptic pattern, with occasional small plaque-like structures in the molecular layer and around the dentate nucleus.

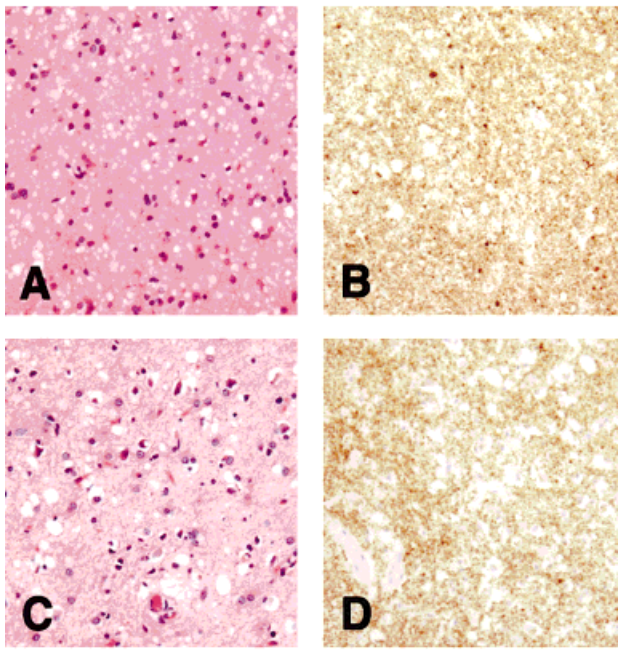

Fig. 1. (A) The frontal cortex in the brain biopsy specimen shows widespread microvacuolar spongiform change, with occasional areas of confluent vacuolation. No plaques are present. Haematoxylin and eosin. (B) Immunocytochemistry for prion protein shows widespread positivity in a reticular (synaptic) pattern in the frontal cortex from the biopsy specimen. No plaques are present. KG9 monoclonal antibody/haematoxylin counterstain following proteinase K digestion. (C) The frontal cortex in the autopsy specimen shows spongiform change, with a coarse pattern of vacuolation. Neuronal loss and astrocytosis are more evident than in the biopsy. Haematoxylin and eosin. (D) Immunocytochemistry for PrP in the frontal cortex in the autopsy specimen shows a widespread synaptic pattern of deposition. No plaques are visible, and there is no evidence of a laminar or perineuronal pattern of PrP accumulation. KG9 monoclonal antibody/haematoxylin counterstain following proteinase K digestion. (A–D) Original magnification ×175.

Western blot analysis of a frozen autopsy sample of the left frontal cortex (the only frozen tissue available) contrasted starkly with that seen at biopsy. The nonglycosylated PrP^{res} was clearly of type 2 mobility (19 kDa); moreover, the glycoform ratio was not characteristic of sCJD and resembled that seen in vCJD (Fig 2). Multiple sampling and analysis from different regions of the available autopsy and biopsy frontal cortex samples ($n = 4$ and 6, respectively) showed a reproducible difference in the glycoform ratio between these 2 samples (Fig 3).

Discussion

All vCJD cases thus far described have been homozygous for methionine at codon 129 of the *PRNP* gene,[4] although this genotype represents a minority of the normal Caucasian population.[11] Comparison with the only other peripherally acquired forms of CJD currently known (iatrogenic CJD and Kuru) suggests that all three codon 129 genotypes might be susceptible to vCJD but that the incubation times could differ.[10,12] Although the codon 129 *PRNP* polymorphism has a major influence in the neuropathology of sCJD, the neuropathological changes in Kuru are modified only to a minor degree by *PRNP* codon 129 polymorphisms.[10,13] Modelling of vCJD in human valine homozygotes using "humanized" mice has suggested that the "glycoform signature" of vCJD will be conserved on a valine background.[9]

The fundamental question posed by this case in the first instance was whether it might represent vCJD in a valine homozygote. These fears were raised by the early onset, long duration, and behavioural symptoms early in the illness without neurological signs. Brain biopsy confirmed the clinical diagnosis of CJD and indicated that the patient had a rare PrP^{res} isotype/codon 129 genotype combination.[11] The clinical features of this case (early onset, long duration, progressive dementia) and clinical test results (normal EEG, cortical abnormalities on MRI) bear a strong resemblance to the four VV1 cases reported.[11,14] The histological features in the brain biopsy are similar to the VV1 cases of sCJD,[11,14] but in the autopsy material there is a closer resemblance to the neuropathology in VV2 cases of sCJD,[11] although no laminar pattern of PrP deposition was identified in any region of the cerebral cortex.

Fig. 2. Western blot analysis of protease-resistant prion protein (PrP^{res}) in frontal cortex from this case at biopsy (b, lane B) and at autopsy (a, lane E). For comparison, the following PrP^{res} types are shown: type 1 from an MM1 case of sporadic Creutzfeldt-Jakob disease (sCJD, lanes A and C), type 2A from a VV2 case of sCJD (lane D), and type 2B from an MM2 case of variant CJD (lane F). Markers are shown (lane G) and their approximate molecular weights indicated in kilodaltons.

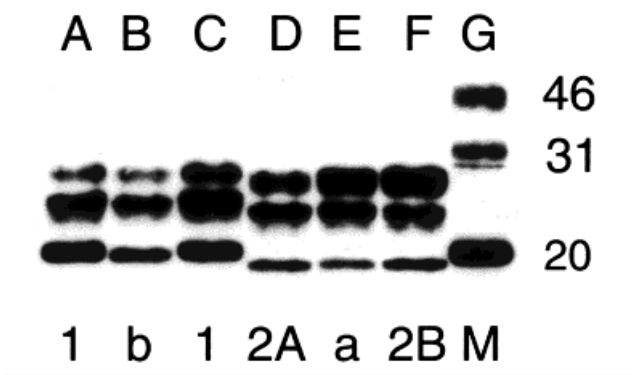

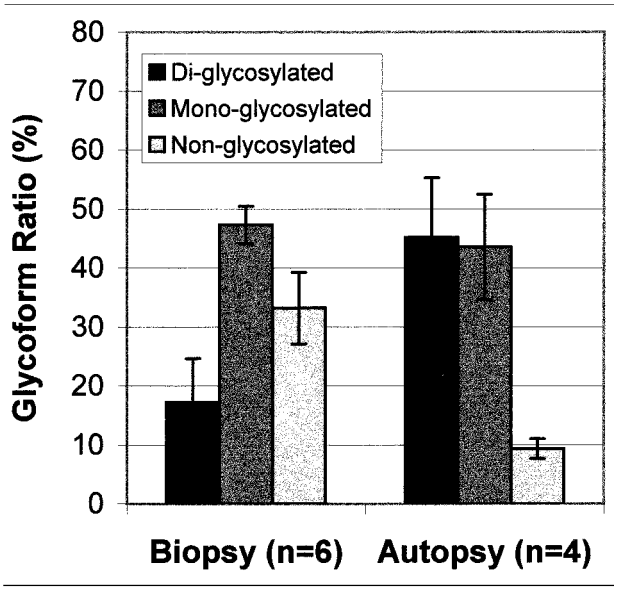

Fig. 3. Histogram showing mean glycoform ratios (%) from multiple samplings and analysis of biopsy (n = 6) and autopsy (n = 4) frontal cortex. Error bars show the standard deviation of the mean.

We therefore believe this case to be sporadic in nature and not related to exposure to BSE. However, the autopsy finding of a PrP^{res} isotype (type 2) and glycoform ratio distinct from that seen in the biopsy is difficult to interpret. Two potential explanations present themselves: (1) disease progression may involve changes in PrP isotype, the single other biopsy/autopsy pair available to us, from a case of vCJD, showing no such difference (data not shown); (2) we may have inadvertently sampled 2 different areas of this brain, which displayed regional variation in PrP^{res} isotype throughout the disease course. Parchi et al.[11] commented that around 3% of sCJD cases contain both type 1 and type 2 PrP^{res} in the cortex. Other estimates are considerably higher (5/14), and it has been further contended that histological heterogeneity correlates with PrP^{res} isotypic heterogeneity.[15] Our own experience indicates that both regional variation in PrP^{res} isotype (1 or 2) and glycoform ratio can occur in sCJD cases.

It is undoubtedly true that the cortical PrP^{res} glycoform ratio can distinguish between sCJD and vCJD in the vast majority of cases.[7,8] However, glycoform ratios resembling those seen in vCJD have been reported previously in fatal familial insomnia,[16] P102L Gerstmann-Sträussler-Scheinker disease,[17] and E200K familial CJD.[18,19] The finding of such a glycoform ratio in this case of sCJD suggests that caution is required in the diagnosis of vCJD on the basis of glycoform ratio in the absence of any other confirmatory evidence.

The UK Department of Health and the Scottish Executive fund the National CJD Surveillance Unit (NCJDSU).

The work of Ms Linda McCardle and her histopathology staff at the NCJDSU is gratefully acknowledged. We also thank Dr W. A. van Gool for performing the 14-3-3 analysis and sequencing the *PRNP* gene, Dr J. Driessen for initial diagnostic workup and referral, Ms T. Koene for the neuropsychological examination, Dr J. Ploegmakers for the brain biopsy and Dr E. Jonkman for the EEG analyses.

References

1. Will RG, Ironside JW, Zeidler M, et al. A new variant of Creutzfeldt-Jakob disease in the UK. Lancet 1996;347:921–925.
2. Bruce ME, Will RG, Ironside JW, et al. Transmission to mice indicate that "new variant" CJD is caused by the BSE agent. Nature 1997;389:498–501.
3. Hill A, Desbruslais M, Joiner S, et al. The same prion strain causes vCJD and BSE. Nature 1997;389:448–450.
4. Will RG, Zeidler M, Stewart GE, et al. Diagnosis of new variant Creutzfeldt-Jakob disease. Ann Neurol 2000;47:575–582.
5. Zeidler M, Sellar RJ, Collie DA. The pulvinar sign on magnetic resonance imaging in variant Creutzfeldt-Jakob disease. Lancet 2000;355:1412–1418.
6. Ironside JW, Head MW, Bell JE, et al. Laboratory diagnosis of variant Creutzfeldt-Jakob disease. Histopathology 2000;7:1–9.
7. Collinge J, Sidle KCL, Meads J, et al. Molecular analysis of prion strain variation and the aetiology of "new variant" CJD. Nature 1996;383:685–690.
8. Parchi P, Capellari S, Chen SG, et al. Typing prion isoforms. Nature 1997;386:232–233.
9. Hill AF, Butterworth RJ, Joiner S, et al. Investigation of variant Creutzfeldt-Jakob disease and other human prion diseases with tonsil biopsy samples. Lancet 1999;353:183–189.
10. Cervenakova L, Goldfarb LV, Garruto R, et al. Phenotypic-genotypic studies in Kuru: implications for new variant Creutzfeldt-Jakob disease. Proc Natl Acad Sci USA 1999;95:13239–13241.
11. Parchi P, Giese A, Capellari S, et al. Classification of sporadic Creutzfeldt-Jakob disease based on molecular and phenotypic analysis of 300 subjects. Ann Neurol 1999;46:224–233.
12. Huillard d'Aignaux J, Costagliola D, Maccario J, et al. Incubation period of Creutzfeldt-Jakob disease in growth hormone recipients in France. Neurology 1999;53:1197–1201.
13. McLean CA, Ironside JW, Alpers MP, et al. Comparative neuropathology of Kuru with the new variant of Creutzfeldt-Jakob disease: evidence for strain of agent predominating over genotype of host. Brain Pathol 1998;8:429–437.
14. Worrall B, Herman ST, Capellari S, et al. Type 1 protease resistant prion protein and valine homozygosity at codon 129 of PRNP identify a subtype of sporadic Creutzfeldt-Jakob disease. J Neurol Neurosurg Psychiatry 1999;67:671–674.
15. Puoti G, Giaccone G, Rossi G, et al. Sporadic Creutzfeldt-Jakob disease: co-occurrence of different types of PrPSc in the same brain. Neurology 1999;53:2173–2176.
16. Telling GC, Parchi P, DeArmond SJ, et al. Evidence for the conformation of the pathologic isoform of the prion protein enciphering and propagating prion diversity. Science 1996;274:2079–2082.
17. Parchi P, Chen SG, Brown P, et al. Different patterns of truncated prion protein fragments correlate with distinct phenotypes in P102L Gerstmann-Straussler-Scheinker disease. Proc Natl Acad Sci USA 1998;95:8322–8327.
18. Hainfeller JA, Parchi P, Kitamoto T, et al. A novel phenotype in familial Creutzfeldt-Jakob disease: prion protein gene E200K coupled with valine at codon 129 and type 2 protease-resistant prion protein. Ann Neurol 1999;45:812–816.
19. Puoti G, Rossi G, Giaccone G, et al. Polymorphism at codon 129 of PRNP affects phenotypic expression of Creutzfeldt-Jakob disease linked to E200K mutation. Ann Neurol 2000;48:269–270.

Frameshift Mutation in the Collagen VI Gene Causes Ullrich's Disease

Itsuro Higuchi, MD,[1] Tadafumi Shiraishi, MD,[1] Teruto Hashiguchi, MD,[2] Masahito Suehara, MD,[3] Takahito Niiyama, MD,[1] Masanori Nakagawa, MD,[1] Kimiyoshi Arimura, MD,[1] Ikuro Maruyama, MD,[1] and Mitsuhiro Osame, MD[1]

Patients with Ullrich's disease have generalized muscle weakness, multiple contractures of the proximal joints, and hyperextensibility of the distal joints. Recently, we found a deficiency of collagen VI protein in two patients with Ullrich's disease. In this study, we detected a homozygous 26 bp deletion in exon 14 of the collagen VI alpha 2 gene (COL6A2) in one patient. This mutation causes a frameshift and a premature termination codon, and results in a truncated collagen VI alpha 2 chain. Our data suggest that at least some cases of Ullrich's disease result from recessive mutations in COL6A2.

Ann Neurol 2001;50:261–265

Ullrich's disease is a unique congenital disorder described as congenital hypotonic-sclerotic muscular dystrophy by Ullrich in 1930.[1] The major clinical findings include generalized muscle weakness and wasting, striking contractures of the proximal joints, hyperflexibility of the distal joints from an early infantile stage, and a progressive course. Muscle biopsies have revealed unequivocal pathological changes of muscular dystrophy.[2,3] Although the gene locus has not been mapped yet, this disease is considered to be a distinct entity of multisystemic involvement inherited as an autosomal recessive trait.[4,5] Recently, we found a complete deficiency of collagen VI in two patients with Ullrich's disease.[6] Our present molecular genetic study confirmed the disease entity of Ullrich's disease, which was called "a forgotten muscular dystrophy" in a previous report.[7]

From the [1]Third Department of Internal Medicine and [2]Department of Laboratory and Molecular Medicine, Faculty of Medicine, Kagoshima University, Kagoshima; and [3]National Okinawa Hospital, Okinawa, Japan.

Received Feb 5, 2001, and in revised form May 7, 2001. Accepted for publication May 9, 2001.

Address correspondence to Dr Higuchi, Third Department of Internal Medicine, Faculty of Medicine, Kagoshima University, 8-35-1 Sakuragaoka, Kagoshima 890-8520, Japan.
E-mail: ihiguchi@med6.kufm.kagoshima-u.ac.jp

Patients and Methods

Patient 1

A 20-year-old male whose parents had no apparent clinical symptoms had neonatal hypotonia and was able to walk supported only between 3 and 5 years old. On examination he showed generalized muscle weakness and atrophy, hyperextensibility of the distal joints, contractures of the proximal joints, a high-arched palate, posterior protrusion of the calcaneus, and kyphoscoliosis (Fig 1). His intellectual development and sensory systems were normal. The serum creatine kinase (CK) was normal. Percent VC (vital capacity) had decreased to 15.8%. Electromyography was myopathic. The clinical course was progressive and the patient underwent tracheotomy because of respiratory failure at the age of 17 years. Muscle and skin biopsy was performed at the age of 20 years.

Patient 2

A 21-year-old male whose parents had no apparent clinical symptoms had neonatal hypotonia and was diagnosed as having congenital dislocation of the bilateral hip joints at 3 months. He was able to sit upright at 3 years but has not been able to walk so far. On examination he showed generalized muscle weakness and atrophy, hyperextensibility of the distal joints, contractures of the proximal joints, a high-arched palate, posterior protrusion of the calcaneus, torticollis, and kyphoscoliosis (see Fig 1). His intellectual development and sensory systems were normal. The serum CK was normal. Electromyography was myopathic. He underwent tracheotomy because of respiratory failure at 14 years old. He has been receiving artificial ventilation during the night since he was 18 years old. Muscle and skin biopsy was performed at the age of 21 years.

As controls, muscle or skin specimens were obtained by open biopsy from patients with various neuromuscular diseases.

Immunohistochemistry

Frozen biopsied biceps brachii muscle specimens and biopsied skin specimens from the two patients and other neuromuscular diseases were cut into 8 μm sections. Besides standard histochemical analysis, an immunohistochemical study was performed on components of the cell membrane and extracellular matrix. The monoclonal antibodies used comprised a 1:100 dilution of collagen III (Chemicon, Temecula, CA), a 1:50 dilution of collagen IV (Boehringer Mannheim, Indianapolis, IN), two kinds of collagen VI (Fuji Chemical, Takaoka, Japan, 1:1000 dilution; ICN Biomedicals, Aurora, OH, 1:100 dilution), a 1:50 dilution of collagen VII (Chemicon), a 1:100 dilution of chondroitin-4-sulphate (Chemicon), a 1:200 dilution of heparan sulfate proteoglycan (Boehringer Mannheim), a 1:1000 dilution of merosin (Gibco BRL, Gaithersburg, MD), and a 1:2000 dilution of

Fig 1. Clinical picture of Ullrich's disease. Generalized muscle atrophy with contractures of proximal joints (A, C), and marked hyperflexibility of distal joints (B, D) in Patient 1 (A, B) and Patient 2 (C, D) with Ullrich's disease.

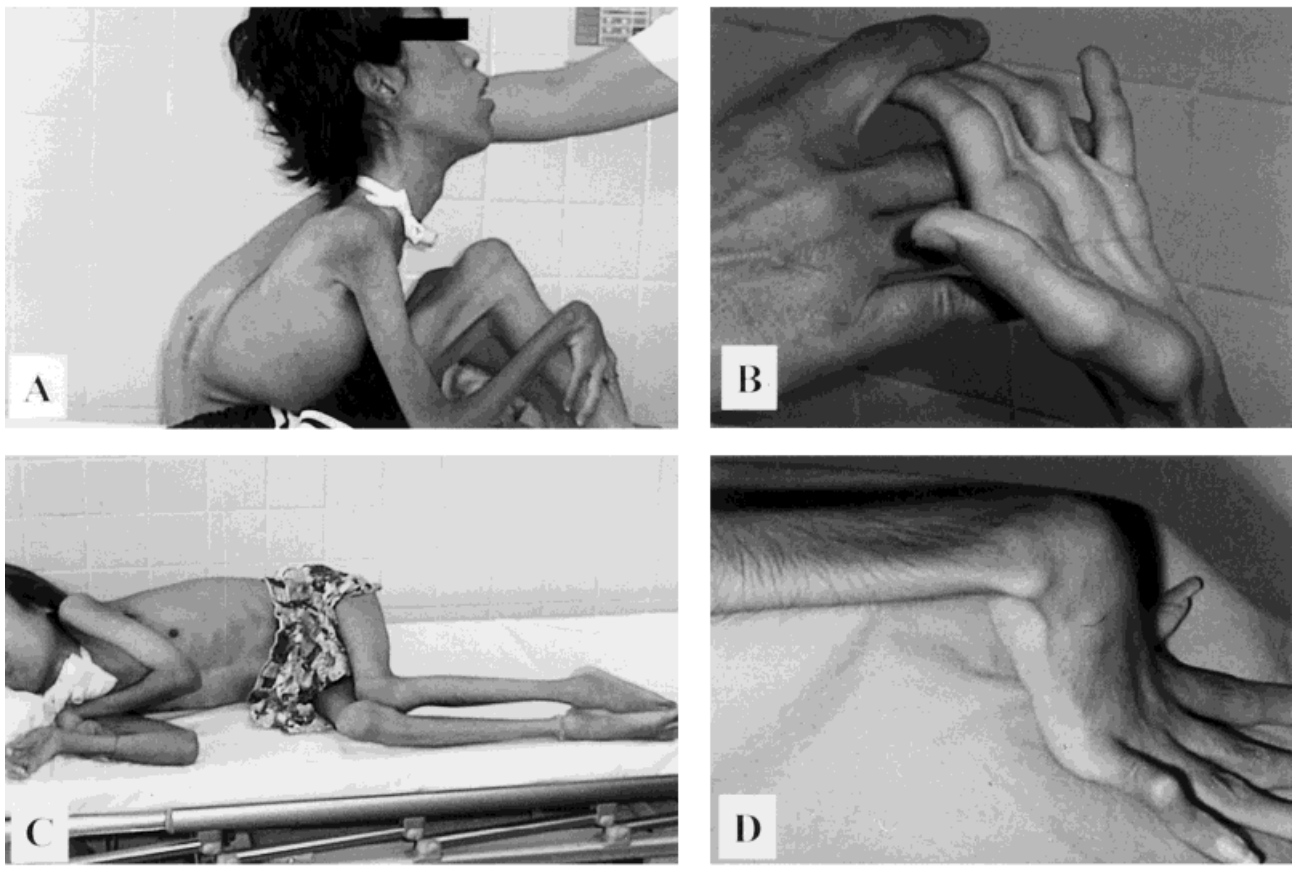

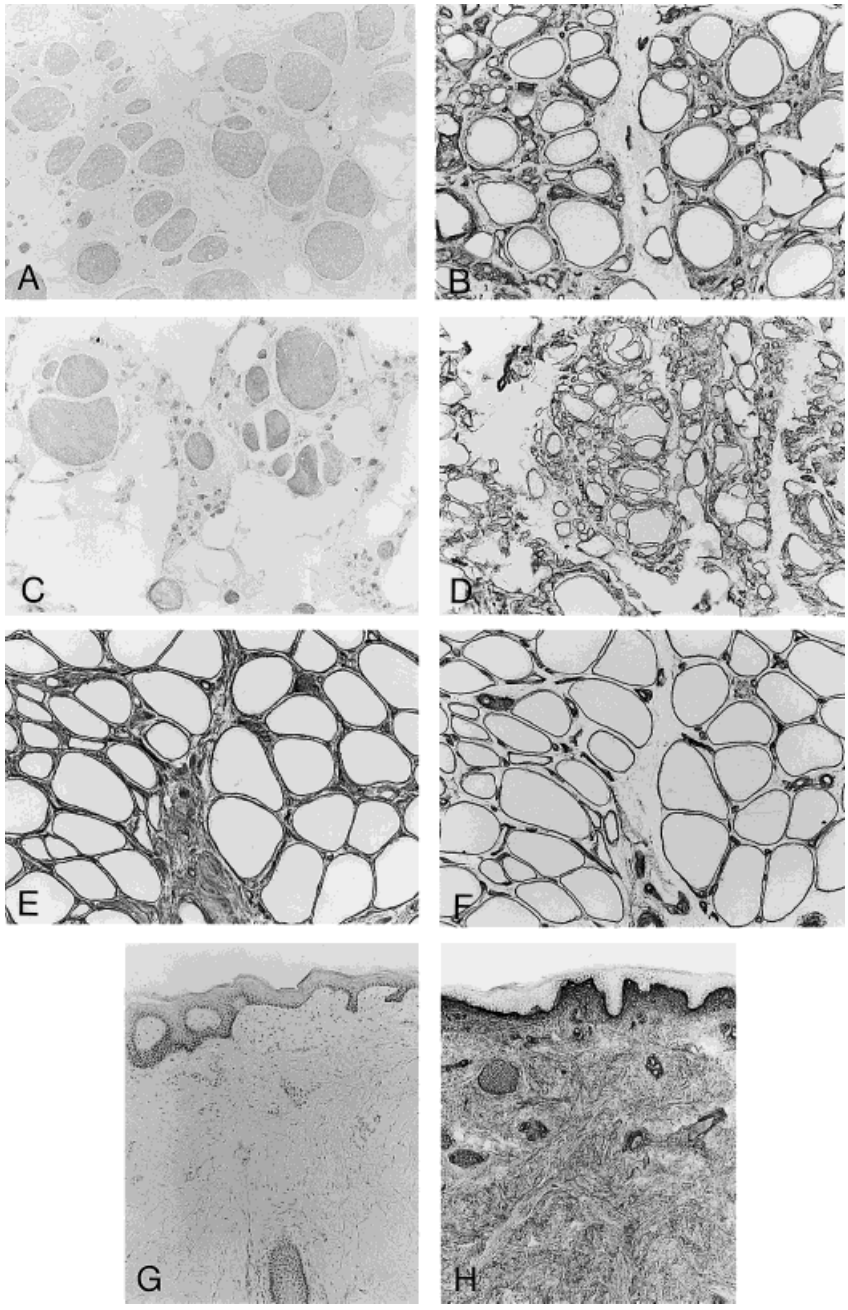

Fig 2. Immunohistochemical staining of biopsied muscle (A–F) and skin (G, H) specimens. Immunohistochemical analysis of collagen VI (A, C, E) and collagen IV (B, D, F) in biopsied muscle specimens from two patients with Ullrich's disease (Patient 1: A, B; Patient 2: C, D), and a patient with Becker muscular dystrophy (E, F). Collagen VI is deficient in the two patients with Ullrich's disease. Collagen IV expression was upregulated in the endomysium of the skeletal muscle specimens from the two patients with Ullrich's disease. Immunohistochemical analysis of collagen VI in biopsied skin specimens from Patient 1 with Ullrich's disease (G) and a patient with Duchenne muscular dystrophy (H). Collagen VI is completely deficient in the patient with Ullrich's disease in contrast to the marked expression in the dermis in the patient with Duchenne muscular dystrophy. ×150.

laminin B1 (Gibco). All immunohistochemical procedures were performed as reported previously.[8]

Collagen VI Mutation Detection

Total cellular RNA of fibroblasts, obtained from skin biopsy specimens, was isolated by the modified acid guanidinium-phenol-chloroform method.[9] The RNA solutions were then used to synthesize cDNA with a first-strand cDNA Kit (Amersham Pharmacia Biotech, Piscataway, NJ). The cDNA solutions were prepared with N6 random primer and reverse transcriptase. The triple helical domains of the three collagen VI genes (COL6A1, COL6A2, and COL6A3) were amplified by polymerase chain reaction (PCR) using three specific pairs of synthetic oligonucleotides per gene, which were designed on the basis of the collagen VI cDNA sequence reported previously.[10,11] The nine sets of primers used were as follows:

388 bp: COL6A11-F-(5′-TCGAATGCCAGCCTGCAAGAGGACC-3′);
COL6A11-R-(5′-TCAGCTCCAGGCTCGCCCTTTTCTC-3′);
355 bp: COL6A12-F-(5′-CCGGCGCCTTTGGACTGAAAGGAGA-3′);
COL6A12-R-(5′-CCCTCATCGCCTCGGTAGCCTTTAG-3′);

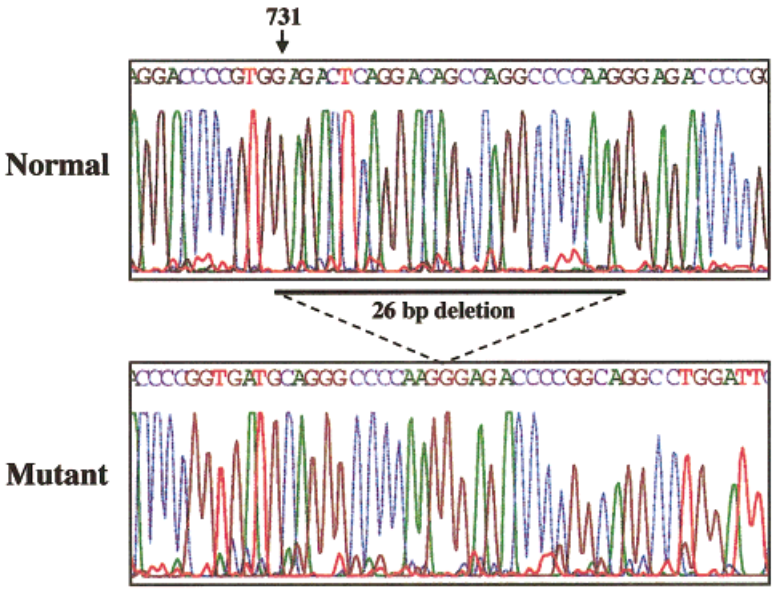

Fig 3. Direct analysis of the nucleotide sequences of COL6A2 cDNA surrounding the deletion in exon 14 in Patient 1 with Ullrich's disease and in a normal control. A frameshift mutation with a deletion of 26 nucleotides from nt 731 to nt 756 can be seen.

388 bp: COL6A13-F-(5′-AGGCTGGCCCTATCGGACC-TAAAGG-3′);
COL6A13-R-(5′-AAAATCTCGCATTCGTCCGGC-CCAG-3′);
472 bp: COL6A21-F-(5′-CTACGGAGAGTGCTACAAG-GTGAG-3′);
COL6A21-R-(5′-ATTGTTGCCTTGATACCCCTT-3′);
524 bp: COL6A22-F-(5′-ATGGACAGAAGGGCAAGC-TG-3′);
COL6A22-R-(5′-TGGCTGTCCTGAGTCTCCAC-3′);
500 bp: COL6A23-F-(5′-GAGAGGTTGGCAACAAAGG-AG-3′);
COL6A23-R-(5′-AGCTGTCGATGACGAAGACC-3′);
400 bp: COL6A31-F-(5′-TTCCCTGCAAGTGCTCTG-GGCAGAG-3′);
COL6A31-R-(5′-TGGCTGTCTTGTCCTGGGTTAC-CCG-3′);
409 bp: COL6A32-F-(5′-GAGATGTTGGGATTCGAG-GGGACCC-3′);
COL6A32-R-(5′-CCGATTCCTCCTTTTGGTCCTG-GCT-3′);
328 bp: COL6A33-F-(5′-TGGGAAGAAAGGGTGAGC-CCGGAGA-3′);
COL6A33-R-(5′-GCACATTGATCGATGGAGTCGCC-CC-3′).

Genomic DNA of leukocytes was also subjected to PCR amplification for COL6A2 genomic fragments using the same primers as those used for the cDNA. The PCR product was separated, purified, and concentrated with a Gel Extraction Kit (Qiagen, Bothell, WA). The cycle sequencing reaction was performed with 10 ng/100 bp of the purified PCR product, using 3.2 pmol of the same primers as those used for PCR amplification. Sequencing was performed with an ABI PRISM dye terminator cycle sequencing kit (PerkinElmer, Oak Ridge, TN). The purified products were run on an ABI PRISM 310 DNA Sequencer (Applied Biosystems, Foster City, CA). As controls in the gene analysis, fibroblasts and circulating leukocytes obtained from normal volunteers were used.

Results

On histochemical examination of the two patients, marked proliferation of fibrous connective tissue, variation in muscle fiber diameter with very small calibered muscle fibers, a fair number of degenerating and regenerating fibers, scarce necrotic fibers, and occasional lobulated fibers were observed. On immunohistochemical examination, collagen VI expression was observed to increase with the proliferation of fibrous connective tissue in other neuromuscular diseases; however, collagen VI expression was completely absent in the skeletal muscle and skin specimens from the two patients with Ullrich's disease (Fig 2). In contrast, collagen IV expression was upregulated in the endomysium and perimysium of skeletal muscle specimens from the two patients with Ullrich's disease (see Fig 2). Other cell membrane and extracellular matrix components examined were all normal in the two patients.

Direct sequencing of both PCR products from cellular RNA of fibroblasts and genomic DNA of leukocytes revealed a homozygous 26 bp deletion in exon 14 of the collagen VI alpha 2 gene (COL6A2) in Patient 1 with Ullrich's disease (Fig 3). This mutation causes a frameshift and a premature termination codon, 169 bp downstream from the deletion, and results in a truncated collagen VI alpha 2 chain, which exhibits impaired assembly and is supposed to be degraded before secretion from the cell. The pathogenetic mutation of collagen VI in Patient 2 with Ullrich's disease has not yet been determined.

Discussion

The most conspicuous pathological finding in the present study was that collagen VI expression was completely deficient in the two patients with Ullrich's disease in spite of the marked proliferation of fibrous connective tissue. The generalized symptoms of Ullrich's disease can be explained by the defect of the collagen VI protein, which shows a widespread distribution in virtually all connective tissues, including skeletal muscle,[12] joint capsules, ligaments, tendons, and skin.[13] Collagen VI is a microfibrillar protein in the extracellular matrix with cell adhesive properties and serves as an anchoring element between collagen I/III fibrils and basement membranes.[14] Many matrix components have been reported to interact with collagen VI.[15] Mutations in the genes that code for collagen VI subunits have been reported in Bethlem myopathy.[16,17] Bethlem myopathy is an autosomal dominant inherited disease characterized by proximal muscle weakness and joint contractures. It has been reported that the expression of collagen VI in Bethlem myopathy is not deficient, and suggested that the disease results from a functional protein haploinsufficiency of collagen VI. Ullrich's disease exhibits no dominant family history and shows marked distal joint laxity and hyperflexibility lasting into the advanced stage, and its clinical course is more severe than in patients with Bethlem myopathy.

A complete deficiency of collagen VI has been reported in a homozygous mutant of COL6A1 knockout mouse as an animal model for Bethlem myopathy.[18] However, the present study suggests that this homozygous knockout mouse should be regarded as an animal model of Ullrich's disease and the milder heterozygous mouse is an animal model of Bethlem myopathy. Interestingly, in the COL6A1 knockout mouse, the most prominent pathological change was observed in the diaphragm, which may be relevant as to the frequent manifestation of respiratory failure in patients with Ullrich's disease.

Although the precise mechanism underlying the dystrophic muscle changes with a deficiency of collagen VI remains unknown, collagen VI play important roles in wound healing in the skin.[19] In the myogenic C2C12 cell line, COL6A2 has been reported to exhibit the same regulation as the MyoD1 and myogenin genes.[20] These data indicate that COL6A2 and the collagen VI protein may be involved in a differentiation or regeneration process in skeletal muscle. In conclusion, our findings suggest that at least some cases of Ullrich's disease result from mutations in COL6A2. They also expand the clinical spectrum of phenotypes associated with the collagen VI gene. This is the first report of a pathogenetic mutation in Ullrich's disease and the first demonstration that a heritable collagen disorder can cause congenital muscular dystrophy.

This study was supported in part by the Research Grant (10A-1) for Nervous and Mental Disorders from the Ministry of Health and Welfare.

We thank Noriko Hirata for her technical assistance.

References

1. Ullrich O. Kongenitale atonisch-sklerotische Muskeldystrophie ein weiterer Typus der heredodegenerativen Erkrankungen des neuromuskularen Systems. Z Ges Neurol Psychiat 1930;126: 171–201.
2. Nonaka I, Une Y, Ishihara T, et al. A clinical and histological study of Ullrich's disease (congenital atonic-sclerotic muscular dystrophy). Neuropediatrics 1981;12:197–208.
3. Goto A, Ishida A, Kobayashi Y, Takada G. A case of Ullrich disease with distinct pathological change of muscular dystrophy. No To Hattatsu 1991;23:289–293 (in Japanese).
4. Furukawa T, Toyokura Y. Congenital, hypotonic-sclerotic muscular dystrophy. J Med Genet 1977;14:426–429.
5. De Paillette L, Aicardi J, Goutieres F. Ullrich's congenital atonic sclerotic muscular dystrophy. J Neurol 1989;236:108–110.
6. Higuchi I, Suehara M, Iwaki H, et al. Collagen VI deficiency in Ullrich's disease. Ann Neurol 2001;49:544.
7. Serratrice G, Pellissier JF. A forgotten muscular dystrophy: Ullrich's disease. Rev Neurol Paris 1983;139:523–525 (in French).
8. Higuchi I, Niiyama T, Uchida Y, et al. Multiple episodes of thrombosis in a patient with Becker muscular dystrophy with marked expression of utrophin on the muscle cell membrane. Acta Neuropathol 1999;98:313–316.
9. Chomczynski P, Sacchi M. Single step method of RNA isolation by acid guanidinium thiocyanate-phenol-chloroform extraction. Anal Biochem 1987;162:156–159.
10. Chu ML, Conway D, Pan TC, et al. Amino acid sequence of the triple-helical domain of human collagen type VI. J Biol Chem 1988;263:18601–18606.
11. Saitta B, Wang YM, Renkart L, et al. The exon organization of the triple-helical coding regions of the human alpha 1 (VI) and alpha 2 (VI) collagen genes is highly similar. Genomics 1991; 11:145–153.
12. von der Mark H, Aumailley M, Wick G, et al. Immunochemistry, genuine size and tissue localization of collagen VI. Eur J Biochem 1984;142:493–502.
13. Hessle H, Engvall E. Type VI collagen. Studies on its localization, structure, and biosynthetic form with monoclonal antibodies. J Biol Chem 1984;259:3955–3961.
14. Kuo HJ, Maslen CL, Keene DR, Glanville RW. Type VI collagen anchors endothelial basement membranes by interacting with type IV collagen. J Biol Chem 1997;272:26522–26529.
15. Bidanset DJ, Guidry C, Rosenberg LC, et al. Binding of the proteoglycan decorin to collagen type VI. J Biol Chem 1992; 267:5250–5256.
16. Jöbsis GJ, Keizers H, Vreijling JP, et al. Type VI collagen mutations in Bethlem myopathy, an autosomal dominant myopathy with contractures. Nat Genet 1996;14:113–135.
17. Pan TC, Zhang RZ, Pericak-Vance MA, et al. Missense mutation in a von Willebrand factor type A domain of the alpha 3 (VI) collagen gene (COL6A3) in a family with Bethlem myopathy. Hum Mol Genet 1998;7:807–812.
18. Bonaldo P, Braghetta P, Zanetti M, et al. Collagen VI deficiency induces early onset myopathy in the mouse: an animal model for Bethlem myopathy. Hum Mol Genet 1998;7:2135–2140.
19. Oono T, Specks U, Eckes B, et al. Expression of type VI collagen mRNA during wound healing. J Invest Dermatol 1993; 100:329–334.
20. Ibrahimi A, Bertrand B, Bardon S, et al. Cloning of alpha 2 chain of type VI collagen and expression during mouse development. Biochem J 1993;289:141–147.

Proton Magnetic Resonance Spectroscopy of Brain Metabolites in Galactosemia

Zhiyue J. Wang, PhD,[1] Gerard T. Berry, MD,[2] Steffi F. Dreha, MD,[3] Huaqing Zhao, MA,[2] Stanton Segal, MD,[2] and Robert A. Zimmerman, MD[1]

Brain edema may occur in infants with galactosemia and has been associated with accumulation of galactitol. Proton magnetic resonance spectra were obtained from 12 patients (four newly diagnosed neonates and eight patients on galactose-restricted diets, age range 1.7–47 years) and control subjects to measure brain galactitol levels in vivo and correlate them with urinary galactitol excretion. The results demonstrate that a markedly elevated brain galactitol level may be present only in newborn infants with galactosemia who exhibit massive urinary galactitol excretion.

Ann Neurol 2001;50:266–269

In patients with galactosemia due to a severe deficiency of galactose-1-phosphate uridyltransferase (GALT), milk feeding in the newborn period may result in a life-threatening toxicity syndrome.[1] Initiation of a galactose-restricted diet will correct the galactose toxicity, but patients still develop long-term complications, including cognitive impairment, speech abnormalities, and primary ovarian failure.[2–4] Because of the block in galactose metabolism, an alternate metabolic pathway becomes active, in which galactose is reduced to galactitol by aldose reductase. The polyol is not further metabolized and is excreted via the kidney.[5] Indeed, excretion of abnormal quantities of galactitol in the urine of galactosemic patients is characteristic of the disorder.[6] Galactitol has been reported to be elevated at autopsy of a patient with brain edema, and the brain contained the highest level of the examined tissues.[7] A high galactitol content in the lens was detected in a GALT-deficient patient with cataract.[8]

Brain abnormalities revealed by magnetic resonance images (MRIs) in patients include diffuse white matter lesions and cerebral and cerebellar atrophy.[9] A brain proton magnetic resonance spectroscopy (^{1}H-MRS) study of six adult patients with galactosemia did not detect galactitol.[10] However, we previously reported brain galactitol accumulation in an infant with encephalopathy and brain edema using in vivo ^{1}H-MRS.[11] To establish the universality of this polyol accumulation, we performed brain ^{1}H-MRS in four neonates recovering from acute galactose intoxication and eight patients who had been on a galactose-restricted diet.

Patients and Methods

Our studies were initiated on a Magnetom SP 1.5T whole-body MRI scanner (Siemens Medical Systems, Iselin, NJ) and continued on two 1.5T Magnetom Vision scanners after machine upgrade. The MRI protocol usually included multislice spin echo proton-density imaging, T1- and T2-weighted imaging, and FLAIR imaging. Patients up to 11 years of age were sedated to obtain motion-free studies. MRS data were acquired using single-voxel STEAM.[12] Regions of interest (ROI) included basal ganglia, occipital gray matter, cerebellar white matter, and parietal white matter. Voxel sizes were typically $1.5 \times 1.5 \times 1.5$ cm^3 for the basal ganglia in neonates and $2 \times 2 \times 2$ cm^3 for all other measurements. Pulse parameters were TR/TM/TE = 1,600/30/20 ms for SP and TR/TM/TE = 1,600/15/10 ms for Vision, 200 to 300 averages. A water reference scan was acquired in each ROI for correcting the eddy current distortion.[13]

The peak area ratios for the galactitol doublet at 3.7 ppm, myoinositol (mI) at 3.55 ppm, choline (Cho) at 3.2 ppm and *N*-acetylaspartate (NAA) at 2.0 ppm to the creatine (Cr) peak at 3.0 ppm were evaluated. Peaks arising from various metabolites overlap each other, and direct integration is not reliable for area measurement. We employed home-written software in interactive data language (IDL) (Research Systems, Boulder, CO) using the LC-model approach for data analysis.[14] The metabolites included in the LC-model were galactitol, mI, glutamine, glutamate, γ-aminobutyric acid, taurine, Cho, Cr, and NAA. The solution spectra of each metabolite were measured under fully relaxed conditions on both SP and Vision systems. The relative contributions of the metabolites to the in vivo data were determined by the LC-model routine and the peak area ratios calculated. Noise in the spectra inevitably introduced errors. It was expected that the least-squares estimation in the LC-model could return a low galactitol level even when there was no galactitol present. Furthermore, the computer routine may have also revealed small negative values that were set to 0.

Twelve patients (6 males and 6 females, age range 6 days to 47 years) with classic galactosemia, defined as absence of GALT activity in red blood cells, were studied (Table). Patients were classified into 2 groups. Group I consisted of 4 neonates (patients 1–4) previously on unrestricted milk ingestion with encephalopathy, liver dysfunction, and massive urine galactitol levels (see Table). Dietary galactose restriction had been initiated, but metabolic perturbations such as high urine galactitol were still present. Group II (patients 5–12) had been on galactose-restricted diets since the neona-

From the Departments of [1]Radiology and [2]Pediatrics, The Children's Hospital of Philadelphia; [3]Metabolic Magnetic Resonance Research and Computing Center, Department of Radiology, University of Pennsylvania, Philadelphia, PA.

Received Mar 29, 2001, and in revised form May 15, 2001. Accepted for publication May 17, 2001.

Address correspondence to Dr Wang, Department of Radiology, The Children's Hospital of Philadelphia, 34th Street and Civic Center Boulevard, Philadelphia, PA 19104.
E-mail: wang@email.chop.edu

Table. Patient Information and Correlation of Galactitol in Urine and Brain

Patient	Age, Sex	Cranial MRI Findings	GALT Genotype	Urine Galactitol (mmol/mol Creatinine)[a]	ROI Location	Galactitol/Cr Area Ratio	Galactitol/Cr and Age of Control[b]
1	6 d, m	Diffusely abnormal WM throughout brain	Q188R/ Q188R	9185	Basal ganglia	5.4	0.00, 8 d
					Occipital GM	12.3	0.00, 7 d
2	9 d, m	Delayed myelination, diffuse WM signal abnormality	Q188R/ Q188R	2784	Basal ganglia	2.12	0.00, 11 d
					Occipital GM	2.42	0.31, 7 d
3	13 d, f	Diffuse symmetric WM signal abnormality	Unknown	2172	Basal ganglia	0.48	0.00, 14 d
					Occipital GM	1.48	0.08, 14 d
4	15 d, m	Subtle diffuse WM signal abnormality	Q188R/ Q188R	6644	Basal ganglia	1.68	0.00, 25 d
5	1.3 y, f	T2WI signal abnormality in subcortical and supratentorial WM	Q188R/ Q188R	195	Parietal WM	0.24	0.00, 1 y
6	1.7 y, f	Ventricular prominence	DEL/ DEL	327	Basal ganglia	0.00	0.00–0.02, 1.3–2.1 y (n = 4)
					Occipital GM	0.00	0.00, 2.5 y
7	9 y, f	Atrophy and diffuse WM abnormalities	Q188R/ unknown	282	Cerebellum	0.00	0.00, 6.1 y
8	13 y, m	Patchy signal increase in T2WI in subcortical and periventricular WM	Q188R/ Q188R	140	Basal ganglia	0.00	0.00–0.10, 9–12 y (n = 2)
9	13 y, m	Mild volume loss	Q188R/ Q188R	162	Occipital GM	0.00	0.00, 8.4 y
10	27 y, f	Supra- and infratentorial volume loss, high signal intensity in FLAIR in periventricular WM	Q188R/ Q188R	199	Cerebellum	0.25	0.00, 30 y
11	30 y, m	Normal	Q188R/ Q188R	124	Basal ganglia	0.01	0.03–0.04, 28–35 y (n = 2)
					Parietal WM	0.01	0.13, 30 y
12	47 y, f	Diffuse WM abnormality and atrophy	Q188R/ Q188R	104	Basal ganglia	0.00	0.00, 41 y

[a]Expected urine galactitol levels for galactosemics under lactose-restrictive diet[6] are age <1 year, 183–800 (normal range 2–78); age 1–6 years, 194–620 (normal range 2–36); age >6 years, 98–282 (normal range 2–19).
[b]When multiple matched control spectra were available, the range of galactitol/Cr, age, and number of control spectra are listed.

WM = white matter; GM = gray matter; T1WI = T1-weighted image; T2WI = T2-weighted image; d = days; y = years; ROI = region of interest.

tal period and had urine galactitol levels, although elevated, within an acceptable range for dietary therapy (see footnotes to Table). Follow-up MRS studies were done for patients 1 and 2 at 4 and 20 months, respectively. However, these results were not used in the statistical analysis.

Twenty-two age-, region-, and scanner-matched control spectra were obtained from 21 healthy adult volunteers and patients who received MRI and MRS examinations for seizure or developmental delay and had negative MRI and blood chemistry findings. Because spectra came from mixed brain regions, a paired Wilcoxon-Mann-Whitney exact test, using *Stat Exact for Windows 3.0* software (CYTEL, Cambridge, MA), was employed to test the differences of metabolite ratios between patients and controls for each group (2-sided $p < 0.05$ considered significant). For this test, patient spectra were paired with control spectra. When multiple control spectra were available for 1 patient spectrum, the average value of each metabolite ratio was entered into the statistical analysis. Information on controls is also listed in the table.

Results

Seventeen patient spectra of good quality (line width < 7 Hz for all and < 4 Hz for neonates) were obtained, excluding those from follow-up studies. The basal ganglia spectra of patient 2 and a control subject together with a galactitol solution spectrum are presented in the figure. In neonatal patient spectra, peaks at 3.67 and 3.74 ppm from galactitol were observed.

The galactitol/Cr ratios and MRS ROI for each patient and matched control are listed in the table. There was a significant increase of the galactitol/Cr ratio in

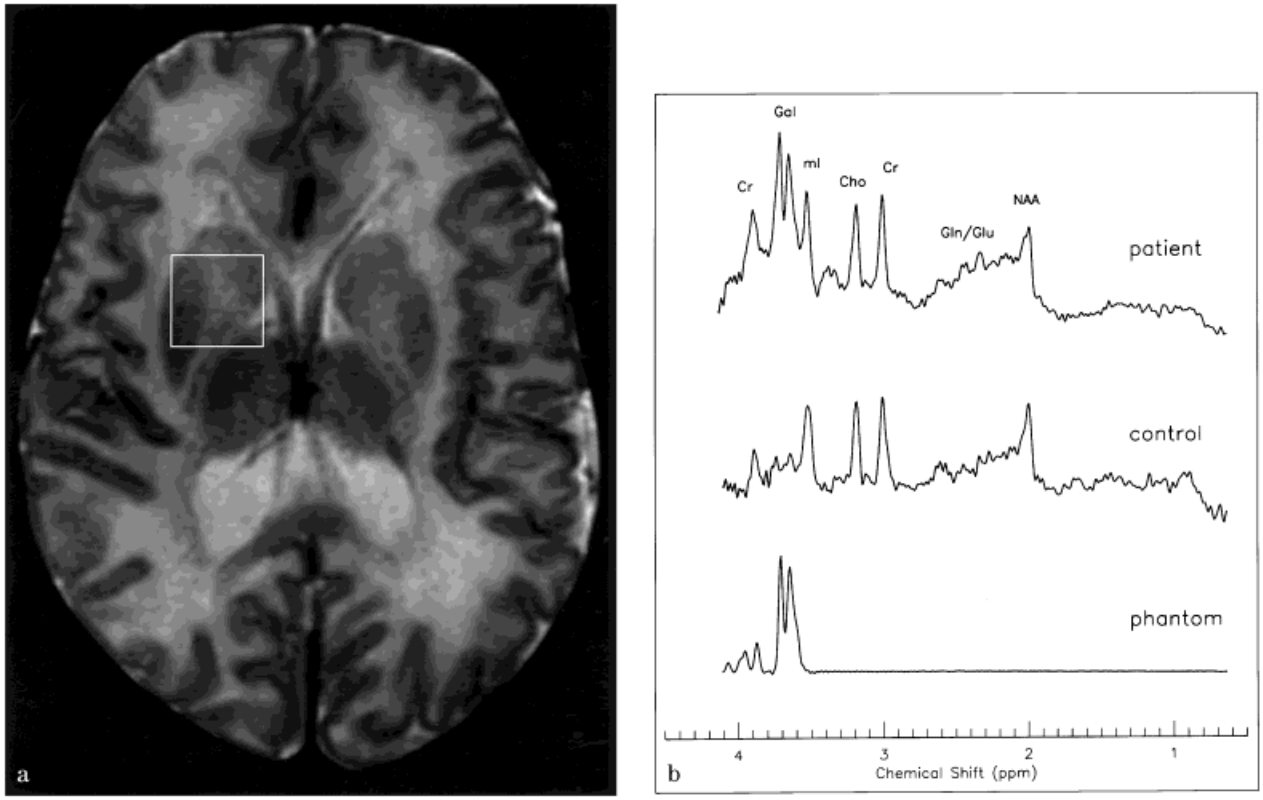

Fig. Magnetic resonance imaging (MRI) and spectroscopy (MRS) of a 9-day-old boy (patient 2) with newly diagnosed galactosemia and acute galactose intoxication. MR examination was performed on a Magnetom Vision 1.5 T scanner using a CP extremity coil. (a) T2-weighted transverse image showing normal basal ganglia and subtly delayed myelination in the internal capsule. Box shows the region of interest for the spectrum of the top trace in b. (b) Spectroscopic detection of galactitol (Gal). Top trace: spectrum from basal ganglia obtained in the same MR examination session as in a. Middle trace: age- and region- matched control spectrum. Lower trace: spectrum of galactitol solution. The patient spectrum shows elevation of galactitol peaks and an increase of glutamine (Gln) and glutamate (Glu) signals. Myoinositol (mI) is slightly reduced. This may be related to the compromised liver function of the patient at the time of the study. Cr = creatine; Cho = choline; NAA = N-acetylaspartate.

group I patients ($p = 0.016$ by paired Wilcoxon-Mann-Whitney exact test). Most patients of group II failed to show a galactitol signal. However, in patients 6 and 11, a slight elevation of signal intensity near 3.7 ppm, consistent with galactitol (galactitol/Cr values of 0.24 and 0.25, respectively), was observed. No significant changes in Cho/Cr, mI/Cr, and NAA/Cr ratios were seen in either group.

In follow-up studies of patients 1 and 2, galactitol was not detected in the brain tissue.

Discussion

Using the galactitol/Cr ratio from the basal ganglia and the urine galactitol level from four neonates, we calculated a Pearson correlation coefficient of 0.83 ($p = 0.125$). This demonstrated a clear trend of correlation between brain and urine galactitol levels. From the galactitol/Cr ratio it is difficult to accurately quantitate the galactitol concentration. An estimate, however, can be made with the assumptions that in neonates the brain Cr concentration is approximately 6.5 μmol/g tissue[15] and that the T1 and T2 relaxation times were similar for the galactitol signals and the 3.0 ppm Cr peak. Since the ratio galactitol/Cr (see Table) is the area ratio and the galactitol and creatine areas represent six and three protons, respectively, the ratio of galactitol concentration to Cr concentration is half the area ratio. This value multiplied by 6.5 μmol/g gives a galactitol range for occipital gray matter of 4.8 to 40 μmol/g and basal ganglia levels from 1.6 to 17.6 μmol/g. These ranges are consistent with the 12.9 μmol/g reported by Wells et al[16] and the 22.18 μmol/g reported by Quan-Ma et al[7] in autopsy studies. Follow-up studies demonstrated normal brain MRS. Whether the presence of detectable brain galactitol in the neonatal period contributes to long-term complications of galactosemia is an open question but should be considered even though brain levels decrease below detection with galactose-restricted diets.

For group II patients, no significant differences between patients and controls were detected. A previous

study estimated that the brain galactitol concentration was below 1 mM, based on ^{1}H-MRS data.[10] If a linear relationship between urine and brain galactitol levels exists, we can estimate the expected range of the brain galactitol/Cr ratio for group II patients. Based on the four basal ganglia observations in group I patients, on average, urine galactitol of 1,000 mmol/mol creatinine corresponds to a galactitol/Cr ratio of 0.47. For group II patients older than six years, the expected urine galactitol range is 98 to 282 mmol/mol Creatinine.[6] This corresponds to a galactitol/Cr range of 0.05 to 0.13. Therefore, possible presence of slightly elevated galactitol levels detectable by MRS in some patients remain a concern. However, advanced MRS techniques, such as two-dimensional spectroscopy, will be needed for reliable and specific measurement of low galactitol levels.

Abnormal MRI findings are common in galactosemia. In our study, nine of 12 patients revealed diffuse white matter signal abnormalities. In most diseases, white matter MRI abnormalities are associated with changes in Cho, NAA and mI levels. However, no alterations of these metabolites were detected in our patients. One explanation may be that only two of the 10 spectra of group II came from white matter regions (0 in group I). Changes in mI/Cr, Cho/Cr, and NAA/Cr ratios, although may be present, did not reach statistical significance. Further studies are needed to investigate changes in these metabolites.

This work was supported by National Institutes of Health grant HDPO1-29847. S. F. D. was supported by the German Scholarship Foundation.

We thank Dr. Suzanne Wehrli for valuable discussions.

References

1. Segal S, Berry GT. Disorders of galactose metabolism. In: Scriver C, Beaudet AL, Sly WS, et al, eds. The metabolic and molecular bases of inherited disease. New York: McGraw-Hill, 1995:967–1000.
2. Waggoner DD, Buist NRM, Donnell GN. Long-term prognosis in galactosaemia: results of a survey of 350 cases. J Inherit Metab Dis 1990;13:802–818.
3. Widhalm K, Miranda da Cruz BDO, Koch M. Diet does not ensure normal development in galactosemia. J Am Coll Nutr 1997;16:204–208.
4. Schweitzer S, Shin Y, Jakobs C, Brodehl J. Long-term outcome in 134 patients with galactosaemia. Eur J Pediatr 1993;152:36–43.
5. Jakobs C, Schweitzer S, Dorland B. Galactitol in galactosemia. Eur J Pediatr 1995;154(Suppl 2):S50–S52.
6. Palmieri M, Mazur A, Berry GT, et al. Urine and plasma galactitol in patients with galactose-1-phosphate uridyltransferase deficiency galactosemia. Metabolism 1999;48:1294–1302.
7. Quan-Ma R, Wells HJ, Wells WW, et al. Galactitol in the tissues of galactosemic child. Am J Dis Child 1966;112:477–478.
8. Gitzelmann R, Curtius HC, Schneller I. Galactitol and galactose-1-phosphate in the lens of a galactosemic infant. Exp Eye Res 1967;6:1–3.
9. Nelson MD Jr, Wolff JA, Cross CA, et al. Galactosemia: evaluation with MR imaging. Radiology 1992;184:255–261.
10. Möller HE, Ullrich K, Vermathen P, et al. In vivo study of brain metabolism in galactosemia by ^{1}H and ^{31}P magnetic resonance spectroscopy. Eur J Pediatr 1995;154(Suppl 2):S8–S13.
11. Berry GT, Hunter J, Wang Z, et al. In vivo evidence of brain galactitol accumulation in an infant with galactosemia and encephalopathy. J Pediatr 2001;138:260–262.
12. Frahm J, Merboldt KD, Hanicke W. Localized proton spectroscopy using stimulated echoes. J Magn Reson 1987;72:502–508.
13. Klose U. In vivo proton spectroscopy in presence of eddy currents. Magn Reson Med 1990;14:26–30.
14. Provencher SW. Estimation of metabolite concentration from localized in vivo proton NMR spectra. Magn Reson Med 1993;30:672–679.
15. Kreis R, Ernst T, Ross BD. Development of the human brain: in vivo quantification of metabolite and water content with proton magnetic resonance spectroscopy. Magn Reson Med 1993;30:424–437.
16. Wells WW, Pittman TA, Wells HJ, Egan TJ. The isolation and identification of galactitol from the brains of galactosemia patients. J Biol Chem 1965;240:1002–1004.

Adult Neuronal Ceroid Lipofuscinosis with Palmitoyl-Protein Thioesterase Deficiency: First Adult-Onset Patients of a Childhood Disease

Otto P. van Diggelen, PhD,[1] Stephane Thobois, MD,[2] Caroline Tilikete, MD,[2] Marie-Thérèse Zabot, PhD,[3] Joke L. M. Keulemans, BS,[1] Patrick A. van Bunderen, BS,[4] Peter E. M. Taschner, PhD,[4] Monique Losekoot, PhD,[4] and Yakov V. Voznyi, PhD[5]

The fluorogenic enzyme assay for palmitoyl-protein thioesterase (PPT) has greatly facilitated the diagnosis of infantile neuronal ceroid lipofuscinosis (Santavuori-Haltia disease) and the search for possible new variants with atypical clinical presentation. Here, we present the first

From the [1]Department of Clinical Genetics, Erasmus University, Rotterdam, the Netherlands; [2]Hôpital Neurologique Pierre Wertheimer, [3]Centre de Biotechnologie Cellulaire, Hôpital Debrousse, Lyon, France; [4]Department of Human and Clinical Genetics, Leiden University Medical Center, Leiden, the Netherlands; and [5]Institute of Organic Chemistry, Moscow, Russia.

Received Apr 3, 2001, and in revised form May 22. Accepted for publication May 24, 2001.

Address correspondence to Dr van Diggelen, Department of Clinical Genetics, Erasmus University, P. O. Box 1738, 3000 DR Rotterdam, the Netherlands. E-mail: vandiggelen@kgen.fgg.eur.nl

cases of adult neuronal ceroid lipofuscinosis with onset in the fourth decade of life due to a profound deficiency of PPT. The causative mutations in the *CLN1* gene were the known, deleterious mutation R151X and the novel missense mutation G108R. Patients presented at onset (31 and 38 years), with psychiatric symptoms only. At present (ages 56 and 54 years), visual, verbal, and cognitive losses have progressed and both patients have cerebellar ataxia and cannot walk without support.

Ann Neurol 2001;50:269–272

The neuronal ceroid lipofuscinoses (NCLs) are a group of inherited, progressive neurodegenerative diseases characterized by lipopigment inclusions in various tissues. At least four clinically distinct NCL forms have been described:[1] infantile- (INCL, Santavuori-Haltia disease; MIM 256730), late-infantile (LINCL, Jansky-Bielschowsky disease; MIM 204500), juvenile (JNCL, Spielmeyer-Vogt disease, Batten disease; MIM 204200), and adult (ANCL, Kufs' disease; MIM 204300). The NCLs are largely diseases of childhood, and ANCL is rare and poorly characterized. Inheritance is autosomal recessive, except for the extremely rare autosomal dominant Parry's disease (MIM 162350). Until recently, classification of subtypes and confirmation of diagnosis were based on the appearance of pathological inclusion bodies, e.g., granular osmiophilic deposits (GRODs) and fingerprint, curvilinear, or rectilinear structures.[1] Over the last six years, several primary defects were discovered, two of which were enzyme deficiencies. A deficiency of palmitoyl-protein thioesterase (PPT) was demonstrated in patients with INCL, caused by mutations in the *CLN1* gene.[2] Mutations in the *CLN2* gene were shown to cause classical LINCL;[3] *CLN2* encodes tripeptidyl-peptidase 1.[4]

Three additional NCL genes have been identified, all encoding membrane proteins with unknown function (*CLN3,*[5] JNCL; *CLN5,*[6] Finnish variant LINCL; *CLN8,*[7] Northern epilepsy or Progressive Epilepsy and Mental Retardation (EMPR)).

We have recently developed a simple fluorimetric enzyme assay for PPT and shown deficiencies in material from patients with INCL;[8] this assay was also used for prenatal diagnosis.[9] Screening of patients with histopathological or clinical symptoms reminiscent of NCL led to the discovery of the presented patients, who have ANCL caused by a deficiency of PPT.

Patients and Methods

Patient 1

Patient 1 (French ancestry, present age 56 years) was referred to the Hôpital Neurologique in Lyon at age 51. She had a previous history of a dysthymic psychiatric disorder since age 31 years without other symptoms. Cognitive regression started at age 45, followed by progressive ataxia and visual dysfunction. Neurological examination at age 51 showed in addition evidence of dementia and bradyphrenia; sluggish motor abilities; a prominent extrapyramidal syndrome associated with hypokinesia; bradykinesia; rigidity and an unstable, flexed posture not responding to dihydroxyphenylalanine (DOPA) therapy. She had a kinetic cerebellar syndrome of the left arm. Deep tendon reflexes, sensory functions, and motor strength were normal. The patient had anosognosia, and her perception of recent events showed temporospatial disorientation and misjudgment. Cognitive evaluation revealed a general impairment: verbal IQ = 73 (Wechsler Adult Intelligence Scale, WAIS), attention span = 4, memory deficit = 27/72 (Signoret's Memory Battery scale), and decreased lexical and semantic fluency. Visual acuity was decreased bilaterally (6/10), but fundi were normal. Magnetic resonance imaging (MRI) showed generalized atrophy, predominantly of the cerebellum and posterior cortex. Electroencephalography (EEG) showed generalized reduced activity, without periodic abnormalities.

Re-examination at age 54 showed further cognitive decline (WAIS verbal IQ = 58, memory deficit = 17/72; Mini-Mental Status score = 19/30) with unchanged extrapyramidal syndrome and cerebellar ataxia. Visual acuity, however, was further decreased (2/10) with a bilateral Piranaud score of 5. Optic atrophy was now prominent, without pigmentary changes. Visual evoked potentials confirmed a bilateral optic neuropathy, whereas electroretinography was normal. Clinical decline was evident, and the patient had visual hallucinations and alternating nystagmus coinciding with periodic occipital activity on EEG. These manifestations indicated focal epileptic activity of the occipital lobe and spontaneously stopped within a week. Lumbar puncture and further neurological investigations were not allowed. Ultrastructural examination of a cutaneous biopsy by electron microscopy showed GRODs in sweat gland cells, which led to the clinical diagnosis of Kufs' disease.

Patient 2

The younger sister of patient 1 (present age 54 years) presented at age 38 years with several episodes of depression without neurological abnormalities and responding somewhat to medication. The only other clear abnormalities were hypertension and an aortic valvulopathy. Between ages 38 and 53, she became progressively bradyphrenic and apathetic, being indifferent to important events in the absence of a clear mood disorder. Memory, speech, and vision declined. At age 53, she was anosognostic and full clinical and neurological examinations indicated a condition similar to that of her older sister: inability to walk or stand up without support due to severe cerebellar ataxia without evident dysmetria, moderate parkinsonism with bilateral rigidity but without tremor, mild myoclonus in the upper limbs, disorientation, and decline of verbal facilities accompanied by frequent perseverations. However, pyramidal signs, chorea, oculomotor abnormalities, and sensory deficit were absent. The Mini-Mental Status score was only 13/30, and the Frontal Assessment Battery score was severely abnormal (Dubois Pillon, 9/21). She was disoriented and unable to summarize her personal history. Verbal fluency and memory were reduced, and she presented with ideomotor apraxia and aphasia. MRI

showed generalized atrophy of the brain, and EEG showed diffuse θ waves without pseudoperiodic triphasic waves. Cerebral blood flow (^{99m}Tc-Ethyl-Cysteinate-Dimer single-photon emission computed tomography) was globally and symmetrically reduced, with a slight predominance in the temporal and parietal lobes. Cerebrospinal fluid was acellular, had normal protein and glucose concentrations, and had no protein 14-3-3 or oligoclonal bands. Tests for Huntington's disease and Leber's disease were negative. Ophthalmological examination showed only bilateral visual loss (2/10). Tests for visual evoked potentials and ultrastructural examinations were not allowed by the patient. A preliminary brief report of patient 2 has been published elsewhere.[10]

Cells and Enzyme Analysis

Fibroblast culture, isolation of peripheral leukocytes, preparation of homogenates, and determination of PPT activity were done as previously described.[8]

DNA Analysis

Genomic DNA (200 ng) was amplified for all 9 exons, including splice sites and at least 20 bp of the intronic sequence. Primer sequences of the mutation-bearing exons (sequences of others are available upon request) were as follows: exon 3F, 5′-TGTAAAACGACGGCCAGTTCAGTGGTTGTTTTCAGTCCC-3′; exon 3R, 5′-CAGGAAACAGCTATGACCTCCCTTCCAAGATAGGTGACA-3′; exon 5F, 5′-TGTAAAACGACGGCCAGTTCTCACAGTGCCTTGTGCAT-3′; exon 5R, 5′-CAGGAAACAGCTATGACCACGGTGTCAGGTCCTGTAATCT-3′.

Results

The clinical report of the probands, 2 sisters 56 and 54 years of age, is presented in Patient and Methods. Disease onset was at 31 and 38 years, respectively, and the clinical/histopathological diagnosis of the elder patient (patient 1) was made 3 years ago, when GRODs were seen in a skin biopsy. This led to the diagnosis of Kufs' disease, and further biochemical studies were not done at that time. A year ago, patient 2 was fully investigated and appeared to have similar clinical signs and symptoms. The fact that her sister had GRODs led to enzyme analysis, and leukocytes and fibroblasts from both patients showed a severe PPT deficiency (table).

Table. PPT Activity in Cells from Probands and INCL Patients

	PPT (nmol/h/mg)	
	Fibroblasts	Leukocytes
Patient 1	8.3, 7.8[a]	1.7, 1.4[a]
Patient 2	8.9, 11[a]	1.0, 1.5[a]
INCL	1.3–9.2 (n = 35)	0.4–1.7 (n = 16)
Controls	96–240 (n = 104)	27–100 (n = 137)

[a]Two independent determinations.

PPT = palmitoyl-protein thioesterase; INCL = infantile neuronal ceroid lipofuscinosis.

Residual PPT activity was in the upper part of the range of INCL patients, consistent with the mild phenotype.

Sequencing of the *CLN1* gene in patient 2 showed the deleterious R151X mutation[11] in exon 5 and a novel missense mutation, G108R, in exon 3 (GGC→CGC). Both mutations were shown in DNA from fibroblasts as well as leukocytes from both patients, indicating compound heterozygosity. This could not be confirmed since both parents are deceased and DNA from the daughter of patient 1 and the two sons of patient 2 was not available for analysis. The G108R mutation was not present in 43 control samples, determined by sequence analysis.

Discussion

Since the primary defect in INCL was demonstrated,[2] it has become clear that classification based on age at onset and histopathology is not unequivocal. Only half the patients with PPT deficiency in the United States and Canada have the severe phenotype characteristic of Finnish INCL, the other half presenting with milder manifestations and onset up to the juvenile age.[11,12] The present probands are now in their sixth decade of life and have widened the clinical spectrum of PPT deficiency greatly. This now includes patients who can be classified as ANCL, indicating the need to abandon the traditional nomenclature of the NCLs, based on onset of the disease. We propose a logical nomenclature of NCLs, directly referring to the genetic classification. Since INCL, LINCL, and JNCL are unofficially often referred to as NCL types 1, 2, and 3, respectively, formalization of this nomenclature would be the best basis to define the clinical entities. The disease NCL1 would then correspond to the gene *CLN1,* NCL2 to *CLN2,* etc. Age at onset could be added as an affix, to specify the subtypes. Our ANCL patients with PPT deficiency would then be classified as NCL1-adult and classical INCL as NCL1-infantile. This revised nomenclature would clarify the confusion regarding the current classification based on age at onset.

Many different mutations have been found in patients with PPT deficiency,[12] indicating that screening for known mutations is not efficient to classify NCL subtypes (except for Finnish INCL). In contrast, our functional enzyme assay screens for all known and unknown mutations in *CLN1.* Therefore, enzyme analysis should always precede mutation analysis in diagnosing new patients. The availability of a simple enzyme assay has led to the discovery of the first adult-onset variant with PPT deficiency, and we expect that awareness of this variant among neurologists will lead to identification of more ANCL patients, who might presently be misdiagnosed.

We thank Dr. Revol for referring Patient 1 to us.

References

1. The neuronal ceroid lipofuscinoses (Batten disease). In: Goebel HH, Mole SE, Lake BD, eds. Biomedical health research, vol 33. Amsterdam: IOS; 1999.
2. Vesa J, Hellsten E, Verkruyse LA, et al. Mutations in the palmitoyl protein thioesterase gene causing INCL. Nature 1995;376:584–587.
3. Sleat DE, Donnelly RJ, Lackland H, et al. Association of mutations in a lysosomal protein with late-infantile neuronal ceroid lipofuscinosis. Science 1997;277:1802–1805.
4. Vines DJ, Warburton MJ. Classical, late infantile neuronal ceroid lipofuscinosis fibroblasts are deficient in lysosomal tripeptidyl peptidase I. FEBS Lett 1999;443:131–135.
5. The International Batten Disease Consortium. Isolation of a novel gene underlying Batten disease CLN3. Cell 1995;82: 949–957.
6. Savukoski M, Klockars T, Holmberg V, et al. CLN5, a novel gene encoding a putative transmembrane protein mutated in Finnish variant late infantile neuronal ceroid lipofuscinosis. Nat Genet 1998;19:286–288.
7. Ranta S, Zang Y, Ross B, et al. The neuronal ceroid lipofuscinoses in human EPMR and mnd mutant mice are associated with mutations in CLN8. Nat Genet 1999;23:233–236.
8. van Diggelen OP, Keulemans JLM, Winchester B, et al. A rapid fluorogenic palmitoyl-protein thioesterase assay: pre- and postnatal diagnosis of INCL. Mol Genet Metab 1999;66:240–244.
9. de Vries BBA, Kleijer WJ, Keulemans JLM, et al. First-trimester diagnosis of infantile neuronal ceroid lipofuscinosis (INCL) using PPT enzyme assay and CLN1 mutation analysis. Prenat Diagn 1999;19:559–562.
10. van Diggelen OP, Keulemans JLM, Kleijer WJ, et al. Pre- and postnatal enzyme analysis for infantile-, late-infantile and adult neuronal ceroid lipofuscinosis (CLN1 and CLN2). Eur J Pediatr Neurol 2001;5:177–180.
11. Das KD, Becerra CHR, Won Yi, et al. Molecular genetics of palmitoyl-protein thioesterase deficiency in the U.S. J Clin Invest 1998;102:361–370.
12. Mole SE, Mitchison HM, Munroe PB. Molecular basis of the neuronal ceroid lipofuscinoses: mutations in CLN1, CLN2, CLN3 and CLN5. Hum Mutat 1999;14:199–215.